Late Cretaceous stratigraphy and paleoceanographic evolution in the Great Australian Bight Basin based on results from IODP Site U1512

K. G. Macleod, L. T. White, C. C. Wainman, Mathieu Martinez, M. M. Jones, Sietske J Batenburg, L. Riquier, S. J. Haynes, D. K. Watkins, K. A. Bogus, et al.

Journal Pre-proof

Late Cretaceous stratigraphy and paleoceanographic evolution in the Great Australian Bight Basin based on results from IODP Site U1512

K.G. MacLeod, L.T. White, C.C. Wainman, M. Martinez, M.M. Jones, S.J. Batenburg, L. Riquier, S.J. Haynes, D.K. Watkins, K.A. Bogus, H.-J. Brumsack, R. do Monte Guerra, K.M. Edgar, T. Edvardsen, M.L. Garcia Tejada, D.L. Harry, T. Hasegawa, R.W. Hobbs, B.T. Huber, T. Jiang, J. Kuroda, E.Y. Lee, Y.-X. Li, A. Maritati, L.K. O'Connor, M.R. Petrizzo, T.M. Quan, C. Richter, G. Tagliaro, E. Wolfgring, Z. Xu

Late Cretaceous stratigraphy and paleoceanographic evolution in the Great Australian Bight Basin based on results from IODP Site U1512

K.G. MacLeod[a], L.T. White[b], C.C. Wainman[c], M. Martinez[d], M.M. Jones[e], S.J. Batenburg[f], L. Riquier[g], S.J. Haynes[h], D.K. Watkins[i], K.A. Bogus[j], H.-J. Brumsack[k], R. do Monte Guerra[l], K.M. Edgar[m], T. Edvardsen[n], M.L. Garcia Tejada[o], D.L. Harry[p], T. Hasegawa[q], R.W. Hobbs[r], B.T. Huber[s], T. Jiang[t], J. Kuroda[u], E.Y. Lee[v], Y.-X. Li[w], A. Maritati[x], L.K. O'Connor[y], M.R. Petrizzo[z], T.M. Quan[aa], C. Richter[ab], G. Tagliaro[ac], E. Wolfring[ad], and Z. Xu[ae]

a- Department of Geological Sciences, University of Missouri, Columbia MO 65211, USA, macleodk@missouri.edu
b- GeoQuEST Research Centre, School of Earth, Atmospheric and LifeSciences, University of Wollongong, Wollongong NSW 2522, Australia, lloydw@uow.edu.au
c- Australian School of Petroleum , University of Adelaide, Adelaide 5005, Australia, carmine.wainman@adelaide.edu.au
d- Univ. Rennes, CNRS, Géosciences Rennes, UMR 6118, Rennes, France, mathieu.martinez@univ-rennes1.fr
e- Department of Geological Sciences, University of Michigan, matthewjones2012@u.northwestern.edu
f- Géosciences Rennes, University of Rennes 1, Bâtiment 15, Campus de Beaulieu, 35042 Rennes, France, sbatenburg@gmail.com
g- Institut des sciences de la Terre de Paris (ISTEP), Sorbonne Université, Paris, France, laurent.riquier@sorbonne-universite.fr
h- Department of Geosciences, Princeton University, Guyot Hall, Princeton NJ 08544, USA, sjhaynes@princeton.edu
i- Earth and Atmospheric Sciences, University of Nebraska, Lincoln NE 68588-0340, USA, dwatkins1@unl.edu
j- Camborne School of Mines, College of Engineering, Math and Physical Sciences, University of Exeter, Penryn, UK, k.bogus@exeter.ac.uk
k- Institut für Chemie und Biologie des Meeres (ICBM), Carl von Ossietzky Universität Oldenburg, D-26111, Oldenburg, Germany, brumsack@icbm.de
l- Technological Institute of Micropaleontology, Unisinos University, Av. Unisinos, 950 - B Cristo Rei, Sao Leopoldo 93022, Brazil, rmguerra@unisinos.br
m- School of Geography, Earth and Environmental Sciences, University of Birmingham, , Edgbaston B15 2TT, United Kingdom, k.m.edgar@bham.ac.uk
n- Camborne School of Mines, College of Engineering, Math and Physical Sciences, University of Exeter, Penryn, UK, T.Edvardsen@exeter.ac.uk
o- Institute for Research on Earth Evolution (IFREE), Japan Agency for Marine-Earth Science and Technology, 2-15 Natsushima-cho, Yokosuka-shi, Kanagawa 237-0061, Japan, mtejada@jamstec.go.jp
p- Geosciences, Colorado State University, Fort Collins CO 80523, dennis.harry@colostate.edu
q- Faculty of Geoscience and Civil Engineering, Institute of Science and Engineering, Kanazawa University, Kanazawa, Ishikawa 920-1192, Japan, jh7ujr@staff.kanazawa-u.ac.jp
r- Department of Earth Sciences, University of Durham, Durham DH1 3LE, United Kingdom, r.w.hobbs@durham.ac.uk
s- National Museum of Natural History, Smithsonian Institution, Washington DC 20560, USA, huberb@si.edu
t- Department of Marine Science and Engineering, China University of Geosciences, Hongshan Street, Wuhan, P.R. China, taojiang@cug.edu.cn
u- Department of Ocean Floor GeoScience, University of Tokyo, 5-1-5 Kashiwanoha, Kashiwa Chiba 277-8564, Japan, kuroda@aori.u-tokyo.ac.jp
v- Faculty of Earth Systems and Environmental Sciences, Chonnam National University, 33 Yongbong-no, Bukgu, Gwangju 61186, Republic of Korea, eun.y.lee@chonnam.ac.kr
w- School of Earth Sciences and Engineering, Nanjing University, Nanjing 210046, P.R. China, yxli@nju.edu.cn
x- Institute of Marine and Antarctic Studies (IMAS), University of Tasmania, Battery Point 7004, Australia, alessandro.maritati@utas.edu.au
y- Department of Earth Sciences, University of Oxford, Oxford OX1 3AN, United Kingdom, lauren.oconnor@univ.ox.ac.uk
z- Department of Earth Sciences, Università degli Studi di Milano, Milano 20133, Italy, mrose.petrizzo@unimi.it
aa- Boone Pickens School of Geology, Oklahoma State University, Stillwater OK 74078, USA, tracy.quan@okstate.edu
ab- Department of Geology & Energy Institute, University of Louisiana, Lafayette LA 70504-0002, USA, richter@louisiana.edu
ac- Institute for Geophysics, Jackson School of Geosciences, University of Texas at Austin, Austin TX 78758, USA, gtagliaro@utexas.edu
ad- Department of Geodynamics and Sedimentology, University of Vienna, Vienna 1090, Austria, erik.wolfgring@univie.ac.at
ae- Institute of Oceanology, Chinese Academy of Sciences, Qingdao Shandong 266071, P.R. China, zhaokaixu@qdio.ac.cn

Abstract: The Upper Cretaceous sedimentary sequence at International Ocean Discovery Program Site U1512 in the Ceduna Sub-basin of the Great Australian Bight represents a continuous, > 690 m thick interval of black silty clay and claystone spanning the lower Turonian through Lower Campanian (~10 million years). Sediments were deposited in an elongate, ~E-W oriented, ~2,500 km long rift system that developed between Australia and Antarctica with an open-ocean connection to the west and a continental bridge to the east. Site U1512 cores provide a unique, continuous record of Late Cretaceous deposition in the Ceduna Sub-basin on the hanging wall of the Wallaroo Fault Zone. Study of U1512 samples could provide both an important high-latitude, southern hemisphere perspective on climatic evolution during the peak and demise of the Cretaceous hothouse and an offshore record of the sedimentation history in the basin during the Late Cretaceous portion of the Gondwanan breakup.

The Upper Cretaceous sequence at Site U1512 is notable for its lithologic uniformity. Burrow-mottled to massive claystone and silty claystone make up the majority of the almost 700 m section, while rare (n = 28) isolated, 2 to 21 cm thick medium to fine sandstone beds are a minor lithology. Macrofossils present include common inoceramids and rare occurrences of other bivalves and ammonites. Microfossils include common occurrences of calcareous nannofossils, agglutinated and calcareous benthic foraminifera, radiolaria and organic-walled dinoflagellate cysts as well as rare small, surface dwelling planktonic foraminifera. Carbonate (<7%) and organic carbon (<1.5%) contents are low. Despite the lithologic uniformity, rhythmic alternations in the intensity of magnetic susceptibility and natural gamma radiation are well-resolved in much of the recovered section and continue through minor coring gaps (as documented by downhole logs). Data from Site U1512 provide new perspectives on our understanding of the deep-water frontier region between Antarctica and Australia.

Introduction

During the Late Cretaceous, the slow separation of Australia and Antarctica led to the development of the Southern Rift System, a ~2,500 km long flooded region of thinned crust that

evolved into an ocean basin (Stagg et al., 1990; Willcox and Stagg, 1990; Totterdell and

Bradshaw, 2004; Direen et al., 2011). Site U1512 was cored during International Ocean

Discovery Program (IODP) Expedition 369 in 3,071 m of water at 34°01.6406'S,

127°57.7605'E. Site U1512 is located in the Ceduna Sub-basin of the Great Australian Bight

near the middle of the rift system (Figs. 1, 2). Recovery was excellent (>90% for the Cretaceous

cores), and U1512 cores provide a 10-million-year-long view of sedimentation and basin

evolution in a relatively offshore position compared to nearby exploration wells (e.g., Totterdell

et al., 2000), the study of which should advance knowledge of Late Cretaceous climate trends,

sedimentation patterns and basin evolution in this part of the Southern Rift System.

Polar regions are a good place to document climate trends as high-latitudes are more

sensitive to climate forcing than low-latitudes. However, there are relatively few high-latitude

paleotemperature records for the Cretaceous, and austral compilations are dominated by data

from the South Atlantic region (e.g., Huber et al., 2002; Huber et al., 2018). Site U1512, at a

paleolatitude of ~65°S at 90 Ma (van Hinsbergen et al., 2015), could provide a new

paleotemperature record useful for testing potential geographical gradients in the timing and

tempo of Turonian greenhouse climate evolution. Neodymium isotopic trends support the

possibility that southern high-latitudes may have become a source region for deep ocean waters

as climate cooled (e.g., Robinson et al., 2010; Murphy and Thomas, 2012; Moiroud et al., 2016;

Huck et al., 2017; Haynes et al., 2020). The semi-restricted region of the rift system cored at Site

U1512 would have potentially been exposed to winter climates conducive to surface water

cooling and sinking, and documentation of seawater Nd isotopic values within the rift could then

be used for tracing circulation patterns in the early stages of Southern Ocean formation.

In this paper, we synthesize shipboard studies and measurements of the cores (Huber et

al., 2019) and discuss their implications relative to regional and global events and trends. We

highlight the positive aspects, initial insights, and remaining challenges related to using these

cores to investigate the Late Cretaceous tectonic, depositional, and climatic history of the

southern Australian margin.

Tectonic history

Mesozoic rifting between Australia and Antarctica led to the development of a network of rift basins along Australia's southern margin called the Southern Rift System. Rifting began in the early Late Jurassic (Oxfordian ~164 Ma) and continued through the end of the Tithonian (~145 Ma) (Stagg et al., 1990; Willcox and Stagg, 1990; Totterdell et al., 2000; Totterdell and Bradshaw, 2004; Direen et al., 2011). Extension led to crustal thinning and the development of a narrow epicontinental seaway between parts of southern Australia and Antarctica (Totterdell et al., 2000; Norvick and Smith, 2001; Sayers et al., 2001; Tikku and Direen, 2008; Boger, 2011; Veevers, 2012; White et al., 2013). This initial episode of rifting led to a basin where Albian–Cenomanian marine deposits accumulated, but it did not progress to the point of producing Jurassic or Early Cretaceous-aged oceanic crust or exhumed mantle.

A second phase of crustal stretching commenced during the Late Cretaceous (Sayers et al., 2001), and from 90 Ma to 30 Ma the seaway developed from a ~2,500 km long continental rift to an ocean basin separating Australia and Antarctica (Stagg et al., 1990; Willcox and Stagg, 1990; Totterdell and Bradshaw, 2004; Tikku and Direen, 2008; Boger, 2011; Direen et al., 2011; White et al., 2013). The initiation of mid-ocean spreading within the rift occurred between 90–84 Ma off the southwestern point of Australia (e.g., Sayers et al., 2001; Tikku and Direen, 2008; Direen et al., 2011) and had progressed well to the east by ~80 Ma (Totterdell and Bradshaw, 2004).

The eastern end of the seaway connected with the Pacific at ~50 Ma. Seafloor magnetic anomalies to the west and south of the South Tasman Rise indicate that the continental connection between Australia and Antarctica was finally broken ~54–45 Ma (Royer and Rollet, 1997; White et al., 2013). Initiation of westward flow of surface waters from the Pacific over the submerged continental crust of the South Tasman Rise at this time is indicated by the distributions of organic-walled dinoflagellate cysts (dinocysts), neodymium isotopic trends, and

sea surface temperature records (Bijl et al., 2013; Scher et al., 2015). However, a fully open, deep water connection through the Tasman Gateway may not have existed until as late as 30 Ma (Scher et al., 2015). Opening of the Tasman Gateway, combined with the opening of the Drake Passage and decreasing atmospheric CO_2 levels, allowed the formation of the Antarctic Circumpolar Current and contributed to the transition from the Eocene greenhouse to the Oligocene icehouse climate state (e.g., Kennett, 1977; Exon et al., 2001; DeConto and Pollard, 2003; Scher et al., 2015; Anagnostou et al., 2016; van den Ende et al., 2017).

Spanning from ~93 Ma to 83 Ma, the lower Turonian through lower Campanian cores recovered at Site U1512 (Huber et al., 2019) represent conditions at the time of renewed Late Cretaceous spreading when an epicontinental seaway flooded much of the thinned crust of the Southern Rift System between Australia and Antarctica. Oceanic crust had begun to form to the SW of Australia during the deposition of the sediments recovered at Site U1512, but deep connections between the western opening of the seaway and the southern proto-Indian Ocean may have been restricted at this time by the Kerguelen Plateau. Eastward, the seaway shallowed and ended at the South Tasman Rise (e.g., Frey et al., 2000; van den Ende et al., 2017). The Ceduna Sub-basin, in which Site U1512 is located, was near the midpoint of this ~2,500 km long, austral E-W-trending seaway (Fig. 2).

Data from onshore sections, seismic imagery, and cuttings from exploration wells provide regional constraints on basin evolution in the vicinity of Site U1512. Late Cretaceous deposition in the region resulted in the accumulation of a series of thick supersequences whose bounding surfaces were controlled largely by tectonic changes in regional sea-level and accommodation space (Totterdell et al., 2000; Norvick and Smith, 2001; Totterdell and Bradshaw, 2004). Sedimentary rocks recovered at Site U1512 correlate closely with the Turonian–Santonian Tiger Supersequence which is composed of marine to marginal marine mudstones up to 4,500 m thick (Totterdell et al., 2000). The Tiger Supersequence and underlying White Pointer Supersequence are interpreted to represent deposition during a breakup phase that occurred after an initial, Early to early Late Cretaceous phase of rapid thermal subsidence and

immediately before a second phase of less rapid thermal subsidence associated with the initiation of slow seafloor spreading in the region (Totterdell et al., 2000; Norvick and Smith, 2001; Totterdell and Bradshaw, 2004). The White Pointer Supersequence is represented by up to 5,500 m of fluvial and marginal marine sediments. Accommodation space for the White Pointer and Tiger Supersequences was created by motion along growth faults. The Tiger Supersequence is overlain by the Santonian–Maastrichtian Hammerhead Supersequence, a series of deltaic deposits up to 5,000 m thick. This deltaic system occupied much of Australia's southern margin and was built of sediments eroded from the eastern highlands of Australia that were transported to the Bight region by a hypothesized Ceduna River (Norvick and Smith, 2001; MacDonald et al., 2013). Site U1512 is located on the hanging wall of the Wallaroo Fault System and is the only continuously cored borehole that has penetrated and recovered Cretaceous rocks in the Great Australian Bight (Fig. 1).

Sedimentology

At Site U1512, a ~10 m thick interval of Pleistocene nannofossil ooze unconformably overlies a well-recovered (>90%), >690 m thick, sequence of dark gray to black, Upper Cretaceous (Turonian–Campanian) silty clay that grades downhole into silty claystone (Huber et al., 2019, Fig. 3). The Cretaceous rocks are dominantly composed of clay minerals, angular silt-sized quartz grains, and trace amounts of feldspar, glauconite, pyrite, dolomite, siderite, mica, and amorphous silica. The abundances and types of authigenic minerals vary throughout the section in no obvious stratigraphic pattern. Biogenic material is absent in some samples, present in most samples, and common (especially inoceramid bivalves) in some samples (Fig. 3). Fabrics present are largely biogenic, and sediments range from pervasively mottled to massive (Fig. 4A-D). There is no apparent stratigraphic regularity to changes in the relative intensity of bioturbation either as progressive trends on the scale of the entire sequence or as alternations over shorter stratigraphic intervals. Bioturbation is present throughout the cored interval

suggesting oxygen was consistently present at the seafloor, but rare, thin (< 0.3 cm) to medium (0.3–0.6 cm) laminations are present below 600 meters below seafloor (mbsf) at the site.

The clay/claystone lithologies are remarkably uniform and dominate the section (>99 % of the total recovered Cretaceous material). In addition, 28 interbeds (2–21 cm-thick) of fine to medium grained glauconitic or sideritic sandstones are distributed irregularly through most of the recovered Late Cretaceous interval but represent <1 % of the total thickness recovered (Fig. 4E, F). Glauconitic sandstone beds are present from 160–330 mbsf; they are moderately sorted and comprised of glauconite and quartz with trace amounts of muscovite, chlorite, siderite and lithic fragments. Sideritic sandstones beds are present from 120–550 mbsf. They are moderately sorted, commonly have a higher quartz content than the glauconitic sandstones, and are cemented with siderite. The two sandstones are lithologically distinct. Beds with large proportions of both glauconite and siderite were not observed. Most sandstones are massive. The general lack of discrete sedimentary structures in these beds could be the result of dewatering, rapid deposition of sediments, lack of variability in grain size, or intense bioturbation. Observed sedimentary features, although rarely present, include normal grading, cross beds, sharp erosional bases, and intraclasts of silty claystone.

Sedimentological observations summarized above suggest that the marine depositional environment was oxygen-depleted, but not anoxic. Sediments were apparently deposited below storm wave base and were isolated from the influence of other processes that would have deposited distinctive beds substantial enough to survive subsequent bioturbation (e.g., substantial turbidity currents, dramatic increases in the relative abundance of biogenic input). Sandstones interbedded with marine mud are typically the result of traction currents or sediment gravity flows, but sedimentary structures indicative of tractive transport or settling are largely absent from the sandstones. Thus, while sandstones at Site U1512 might result from traction currents or sediment gravity flows. there is not direct observational support for these processeses. Alternative possible mechanisms that could explain the occurrence of the sandstones of Site

U1512 are winnowing or condensed deposition, processes that might concentrate the authigenic phases that comprise most of the the grains in these beds.

The dominance of silty clays and silty claystones at this site interrupted by only a small number of thin sandstone interbeds that lack of any indication of storm activity support quiet water deposition throughout the recovered interval. Sedimentation rates are quite high on average (~700 m deposited in ~10 million years), and show a trend from high values of up to 120 m/myr during the early Turonian down to more modest values of ~25 m/myr during the Coniacian through early Campanian (Fig. 3).

Paleontology

Calcareous nannofossils provide the most refined biostratigraphic control for Hole U1512A and indicate deposition spanning the early Turonian (Subzone CC10c) to the late Santonian to early Campanian (Zone CC17) of Perch-Nielsen (1985). Coniacian to lower Campanian calcareous nannofossils are characterized by moderately preserved assemblages exhibiting lower diversity than coeval open oceanic sections. Differentiation of Santonian Zones CC16 and CC17 is difficult due to the nearly complete lack of holococcoliths (a feature this sequence shares with correlative sediments in the Western Interior Basin of North America (Watkins et al., 1993; Kita et al., 2017). The Turonian-Coniacian interval in Hole 1512A appears to be stratigraphically complete, including the presence of uppermost Zone CC13 containing *Micula cubiformis* and *Marthasterites furcatus,* but lacking *Micula staurophora*. Sediment accumulation rates for the Coniacian to lower Campanian average 25 m/myr and suggest relatively normal hemipelagic sedimentation with suboptimal surface water mass conditions. High quantities of the diminutive *Repagulum parvidentatum* indicate a strong austral influence and suggest elevated surface water productivity (Watkins et al., 1996). This Coniacian to lower Campanian sequence is separated from a lower interval containing Turonian nannofossil

assemblages by approximately 100 m of dark, non-calcareous mudstones. The lower nannofossil-bearing interval encompasses Subzone CC10c through much of Zone CC12 (Perch-Nielsen, 1985) and, similar to the Coniacian to lower Campanian sequence, contains moderately-preserved, relatively low diversity assemblages missing several taxa generally characteristic of open ocean settings. Sediment accumulation rates for the lower interval average 120 m/myr and indicate much higher rates of terrigenous clastic influx during the Turonian than during the Coniacian to early Campanian (Fig. 3). Age constraints from other foraminifera, radiolaria, and dinoflagellate cysts are consistent with the nannofossil-based age estimates but do not refine these dates.

Planktonic foraminifera are quite rare and are dominated by small (<150 um) specimens of inferred shallow water dwellers (e.g., *Planoheterohelix*, *Whiteinella* and *Muricohedbergella*). Double-keeled taxa such as the dicarinellids and falsotruncanids, which are generally inferred to be thermocline dwelling, are almost completely absent. The assemblage present may indicate the absence of a suitable (sub)thermocline depth habitat perhaps due to one or more of the following factors: shallow water depth, relatively nearshore location of the site, salinity markedly higher or lower than normal marine conditions and/or a shallow or expanded oxygen minimum zone (Falzoni et al., 2016; Huber et al., 1995; 2018). The abundance of 'opportunistic' biserial taxa supports the hypothesis that of 'stressed' surface waters throughout the Late Cretaceous at this site such as meso-eutrophic conditions or non-normal marine salinity waters (Leckie et al., 1998).

Terrestrial plant debris is present in many samples. Radiolaria are sporadically present above 600 mbsf and occur in most samples above 450 mbsf. Large (>45 µm) dinocysts, which were present in the foraminiferal preparation residues, on the other hand, are largely restricted to samples from below 450 mbsf. The (rare) presence of *Palaeohystrichophora infusorioides* throughout the Cretaceous sequence supports age estimates based on nannofossils. It should be

noted, though, that shipboard dinocyst observations are preliminary, as preparation procedures used are likely to miss many individuals and taxa.

Other fossils present in the cores are benthic foraminifera, radiolaria, sponge spicules, dinocysts, inoceramids, and fish scales, fish bones, and fish tooth fragments. Among these, inoceramids are most common. Inoceramids occur both as isolated prismatic shell fragments as well as intact shells that are wider than the core (Fig. 5). Inoceramids are common globally in Late Cretaceous bathyal samples (MacLeod et al., 1996; MacLeod and Huber, 2001). They are known to have tolerated or even preferred suboxic to dysoxic environments (e.g., Elder, 1985; MacLeod and Hoppe, 1992; MacLeod, 1994; Kauffman et al., 2007) and have been reported from dominantly anoxic settings (Henderson, 2004; Jiménez Berrocoso et al., 2008).

Benthic foraminifera are present in more than half of the samples examined and are generally dominated by agglutinated taxa including abundant tubular forms (e.g., *Kalamopsis grzybowski*, *Ammodiscus* spp.) and frequent specimens of *Haplophragmoides* spp., *Ammobaculites* spp. and trochamminids. The most common calcareous benthic taxa are *Gavelinella* sp., *Cibicidoides* spp., *Gyroidinoides* spp. as well as members of the Dentalina/Nodosaria group. All these taxa are usually associated with deposition at bathyal to abyssal water depths (Tjalsma and Lohman, 1983; van Morkhoven et al., 1986; Kaminski and Gradstein, 2005). Whereas calcareous benthic foraminifera are rare throughout the Cretaceous cores, they display relatively low taxonomic diversity in younger samples consistent with deepening upsection (Huber et al., 2019). Finally, miliolid foraminifera were observed in a few samples (U1512A 27R – 29R, 259-277 m, U1512A 69R, ~662m). This group shows its highest abundance in outer shelf environments (Holbourn and Moullade, 1998; Gräfe and Wendler, 2003) but has a broad bathymetric range. We also can not rule out downslope reworking.

Trace fossils present (*Chondrites, Planolites, Zoophycos,* and *Thalasinoides*) are generally associated with relatively deep settings, and the high abundance of agglutinated benthic foraminifera combined with the general scarcity of calcareous microfossils could be interpreted as indicating deposition at abyssal depths under corrosive bottom waters, (i.e., below

the carbonate compensation depth (CCD). Calcareous fossils, most notably nannofossils and inoceramid bivalves, are consistently present, however, ruling out deposition below the CCD with the possible exception of a barren interval at 200–300 mbsf. Further, whereas benthic fossils (macro-, micro-, and trace) are consistent with deposition at bathyal or greater depths, similar assemblages can also be found at depths < 300 m in the Western Interior Seaway (WIS) of North America in the Late Cretaceous (Sageman, 1989; Savrda and Bottjer, 1989; MacLeod and Irving, 1996; Sageman and Bina, 1997).

Overall, paleontological data support deposition within a relatively restricted, low oxygen, relatively deep setting (inferred based on the absence of shallow water benthic foraminifera or other fossil indicators of deposition at shelfal depths). Trends in relative abundance among and within groups are consistent with a general deepening up section, but additional work including detailed observations of radiolaria and dinocysts are needed to refine and strengthen paleoceanographic and biostratigraphic conclusions.

Geochemistry

Below the Pleistocene ooze at the top of the section, the 690 m-thick Cretaceous silty claystone shows consistently low carbonate content (generally <7%) and modest total organic carbon (TOC) contents (<1.5%) (Huber et al., 2019, Figure 6). Organic carbon present is dominated by Type III kerogen (indicative of terrestrial origin), based on the hydrogen and oxygen index values (21–52 and 49–61, respectively). Organic carbon content is similar to the 1–2% TOC values reported for samples from exploration wells on the shelf for the White Pointer and Tiger Supersequences, but higher TOC values (4–7%) have been reported for samples dredged near Site U1512 (Totterdell et al., 2000; Totterdell and Mitchell, 2009).

Owing to the availability of metabolizable organic matter, sulfate is essentially consumed by bacterial sulfate reduction within the top 100 m of the sedimentary column. This depletion in sulfate is accompanied by concomitant increases in dissolved barium due to the dissolution of biogenic barite (Torres et al., 1996). Pore-water trends suggest that the sulfate/methane transition

is located around 100 mbsf. In addition, porewater concentration decreases in potassium and magnesium and increases in calcium suggest ongoing alteration of a volcaniclastic component within the sedimentary column, while silicon values reflect the presence of a biogenic silica component, most likely opal A (Huber et al., 2019).

Methane dominates gas components in the middle third of the formation (~300-450 mbsf) suggestive of *in situ* (biogenic) methanogenesis, an inference supported by an increase in the methane to ethane ratio to values >1000 (e.g. Whiticar, 1994; Smith and Pallasser, 1996; Strąpoć et al., 2008 and references within, Fig. 6). This interval is also associated with slightly lower TOC to total nitrogen (TN) ratios, possibly reflecting carbon loss via methanogenesis as the kerogen type suggests this variation in TOC:TN is not related to changes in terrestrial input. Below ~470 mbsf, the methane to ethane ratio decreases markedly suggesting the possibility of thermogenesis (Pimmel and Claypool, 2001; Huber et al., 2019); however, the low thermal maturity of these sediments suggests it is unlikely this gas was formed *in situ*. Upward migration of thermogenic hydrocarbons would be consistent with the presence of rocks with relatively high TOC values (Totterdell et al., 2000; Totterdell and Mitchell, 2009) deeper in the stratigraphic section.

Petrophysics and Magnetostratigraphy

Measurements of natural gamma radiation (NGR, a property that results from the radioactive decay of ^{238}U, ^{232}Th and ^{40}K) and magnetic susceptibility (MS, a metric of the degree to which minerals present are magnetized by an imposed magnetic field) exhibit large changes over stratigraphic thicknesses ranging from meters to 100's of meters (Fig. 7). This obvious variability in physical properties stands in stark contrast both to the general uniformity of sediment composition and fabric and to the only broad and subtle trends in fossil content. Average NGR and MS values generally exceed 25 counts per second (cps) and 6 Instrument Units (IU), respectively, on long length scales as shown by LOWESS curves with high α-values (Fig. 7). However, two prominent excursions to lower NGR and MS values occur at ~340 and

~680 mbsf, likely due to a decrease in the content of clay minerals, which are paramagnetic and traditional carriers of radiogenic elements (Quirein et al., 1982; Hunt et al., 1995). Similarly, two potentially correlative decreases in NGR occur in the Tiger Supersequence of the Potoroo-1 well, north of Site U1512 in the Eyre Sub-basin (Totterdell et al., 2000). The deeper decrease in NGR at Potoroo-1 occurs near the base of the Tiger Supersequence, suggesting that coring at Site U1512 penetrated the majority of this regional Upper Cretaceous depositional sequence. The shallower decrease in NGR in the middle portion of the Tiger Supersequence at Potoroo-1 marks an unconformity inferred from regional seismic data (Totterdell et al., 2000), which may extend to Site U1512 (~340 mbsf) either as a cryptic hiatus or correlative conformity. On shorter length scales, 1–8 m thick alternations of variable amplitude in NGR and MS are superimposed on larger scale shifts in average values. The Upper Cretaceous interval displays seemingly rhythmic oscillations of NGR and MS values that are well-resolved, in phase, and positively correlated, particularly between 105–180, 310–410, and 590–700 mbsf (Fig. 7). The shortest scale of variations, appearing as spikes in the data, often correlate with sandstone intervals, intervals with pyrite nodules, siderite, and/or concentrations of inoceramid shells.

The variability in NGR and MS measurements through the Site U1512 section is unexpected given the lithologic uniformity. Lithologic monotony implies relative environmental constancy, but the rhythmic oscillations of NGR and MS at Site U1512 indicate more dynamic conditions in the system. Because the sediments are dominated by terrigenous material, changes in weathering and/or erosion in the source regions influencing the mineralogy of the sediments seems the most likely cause of the cyclic variation, but hanges in grain size or mineralogical composition are difficult to observe in these thoroughly bioturbated, fine grained sediments.. Rhythmic variation in silt to clay ratios could reflect subtle changes in the depositional environment whereas the relative portion of different minerals in the clay size fraction could be forced by changes in weathering intensity in source areas paced by Milankovitch cycles and recorded by the NGR and MS signals. Thus, understanding the source of NGR and MS variability in samples from Site U1512 could provide a perspective on terrestrial conditions

during peak Late Cretaceous greenhouse times at southern high latitudes, or alternatively if the NGR and MS variations reflect alternations in sediment grain size, on sorting and transport processes in the oceanic realm. As noted above, the occurrence of thin sandstone beds suggests either episodes of traction transport, winnowing, and/or condensation episodically influenced the local seafloor.

Preliminary spectral analysis of the NGR signal from 105 to 180 mbsf detects a significant high amplitude peak between ~0.2–0.4 cycles/m (Fig. 7), suggesting a periodic driver of cyclicity in the record as opposed to forcing by stochastic processes. This inference supports the assertion that Milankovitch cycles, and, thus, climatic cycles drove cyclic sedimentary patterns reflected in oscillating NGR and MS values. Future cyclostratigraphic analyses in additional Late Cretaceous intervals at Site U1512 are needed to rigorously test this hypothesis.

Paleomagnetic polarity is dominantly normal, which is consistent with biostratigraphic age estimates (Fig. 3). In the upper 200 m of recovered material polarity is uncertain; thus, the shipboard preliminary paleomagnetic data are not helpful in refining placement of Santonian-Campanian boundary. A short reversed interval between 256 and 259 mbsf (Huber et al., 2019) is tentatively interpreted as a field excursion during the Cretaceous Normal Superchron (C34n). Core disturbance (principally biscuiting) in the upper ~80 m and deviation of the borehole from vertical in the deeper parts of the hole (>500 mbsf) compromise interpretation of the magnetic inclination data.

Downhole Geophysics

As well as shipboard measurements of physical properties, the hole was logged to measure *in-situ* values including natural gamma, p- and s-wave velocities, and hole deviation (Fig. 8). The natural gamma values showed a good correspondence to those measured from the recovered cores (Fig. 7). The p-wave trend shows a general increase in velocity with depth as would be expected due to compaction, but the s-wave velocity trend is more complex with an interval of lower velocities between 240 and 270 mbsf that coincides with the level of one of the

few cores (21R) with poor recovery (Figs. 3, 8). Below 410 mbsf, s-wave velocity drops again but largely recovers by 570 mbsf. These lower s-wave velocities are correlated with higher natural gamma and the highest sedimentation rates (~120 m/myr). Finally, it is also noted that there is significant deviation of the hole from vertical which by 650 mbsf had reached an angle of 27° which result in cumulative error in true depth is >13 m by the bottom of the hole with most of that excess occurring between 500 and 700 mbsf.

Discussion

The excellent recovery of Upper Cretaceous rocks achieved at IODP Site U1512 (>90%), and the deeper and more basinward position (relative to existing wells) of this site within the Great Australian Bight makes the new cores a novel, potentially important, archive of Late Cretaceous conditions in the region. The lower Turonian rocks from the base of the recovered sequence were deposited within the warmest portion of the Late Cretaceous greenhouse climate, and deposition continued through to the early Campanian by which time Earth had cooled significantly (e.g., Huber et al., 2018; O'Connor et al., 2019). The sediments also span the time of expected initiation of seafloor spreading within the western to central portions of the Southern Rift System and are partially coeval with thick marine shales in the Otway Basin to the east (Gallagher et al., 2005). The high proportion of detrital material including terrestrial plant matter in a marine sequence could allow relationships between terrestrial and marine climate to be investigated. Important questions regarding the depth, depositional environment, sedimentation rates, and completeness of the record, though, need to be addressed to realize the potential of Site U1512 cores.

Details of the depositional environment are difficult to uniquely interpret as existing data suggest divergent interpretations. The benthic foraminifera present, the general scarcity of calcareous fossils, lack of physical sedimentary structures, and fine grain sizes suggest deep water deposition whereas high sedimentation rates, dominance of terrigenous sediment, the presence of woody plant debris, and the planktonic foraminiferal assemblage present suggest a

relatively proximal setting. The relatively narrow N-S width of the seaway and progressive deepening as seafloor spreading propagated eastward could help explain the presence of these seemingly contradictory observations within the same sequence, and specifics of the basin (e.g., partial restriction and estuarine conditions, trapping of coarse terrigenous materials in delta deposits) could reduce the role of depth in controlling sediment character and fossil content.

Prior to the initiation of seafloor spreading, the Southern Rift System was effectively an epicontinental seaway spanning 2,500 km from Cape Leeuwin in the west to the Tasman Rise in the east (Fig. 2). Due to high sea levels in the Late Cretaceous (~200 m above modern day heights; e.g., Hardenbol et al. (1998), epicontinental seas were common. However, none of these areas are obvious parallels for the Southern Rift System. The chalks of NW Europe were developed on flooded passive margins and are dominated by calcareous, biogenic sediments. The flooded margins of South America, North Africa, and the North American Atlantic and Gulf coastal plain accumulated considerable terrigenous material but lack the apparent oceanographic restriction present at Site U1512. As an elongate seaway with relatively narrow, restricted connections to adjacent ocean(s), the Southern Rift System most closely resembles the Late Cretaceous North America Western Interior Seaway (WIS) in scale and gross geometry. Indeed, offshore marine facies of the WIS show many similarities to Turonian–Santonian sediments at Site U1512 including fine-grained deposits that are pervasively bioturbated with changes among *Chondrites, Planolites, Zoophycos, and Thalasinoides* ichnofacies providing a record of paleo-oxygenation (Savrda and Bottjer, 1989). Also similar to Site U1512, there are low abundances of planktonic foraminifera with an absence of keeled forms in many coeval units of the WIS (Lowery et al., 2017) and inoceramids flourished in places in the variably oxygenated seaway (Elder, 1985; MacLeod and Irving, 1996; Sageman and Bina, 1997). Finally, astronomically paced climate cyclicity played an important role in governing depositional environment conditions, carbon cycling, and bedding patterns in the WIS (Sageman et al., 1997), as may be the case at Site U1512 based on oscillations of NGR and MS (Fig. 7).

There are, however, important differences between the WIS and this southern epicontinental seaway. The WIS formed over a continental flexure due to orogenic loading during the Sevier orogeny (Jordan, 1981; Pang and Nummedal, 1995) and had maximum water depths of a few hundred meters. The WIS had drained by the early Paleogene. The Australian Southern Rift System, in contrast, evolved from its epicontinental stage to an ocean basin by the end of the Paleogene. Maximum sedimentation rates in the offshore calcareous mudstones of the WIS generally do not exceed 25 m/myr in the basin center (e.g., Locklair and Sageman, 2008), whereas they exceed 120 m/myr in the carbonate-lean Turonian section of Site U1512 and were higher in other exploration wells on the southern Australian margin (e.g., Totterdell et al., 2000; Gallagher et al., 2005). Thus, any early Turonian Southern Interior Seaway (SIS) phase of the Southern Rift System was a deeper, darker, and more rapidly accumulating sibling, not a twin, of the WIS. Comparison between the two, though, could be used to test models of circulation, sedimentation, and ecology within such elongate seaways as well as to examine the importance of flow between the seaways and adjoining oceans to regional paleoceanography.

From 93–83 Ma, sedimentation rates at Site U1512 slowed by a factor of five, radiolaria replaced dinocysts in the microfossil assemblages, and benthic foraminifera show a relative increase in calcitic forms. These shifts correlate with eastward progression of mid-ocean spreading into the region by ~84 Ma (Sayers et al., 2001). If subsidence and growth faults on the shelf trapped an increasing portion of the sediment input to the basin while motion on the Wallaroo Fault System continued, there could have been deepening at Site U1512 without a significant change in sediment character.

If significant deepening at Site U1512 occurred from the late Turonian onward, it should be apparent in both details of the microfossil assemblages and in sedimentation rates. Among microfossils, better documentation of dinocysts and radiolarian assemblages could provide additional constraints on changing water depths. A deepening model leads to the prediction that the dinocyst species observed as largely restricted to the lower and middle Turonian portions of the sequence would show a preference for coastal or nearshore environments while the radiolaria

most abundant in late Turonian and younger levels of the cores would have a more open ocean aspect. Stratigraphic trends in the species present within these groups should show the same progression. In addition, there should be a geographic difference in assemblage patterns with the dinocysts remaining abundant (and radiolaria being relatively rare) throughout the Tiger Supersequence in shelfal settings (e.g., samples from the Jerboa-1 well) where sedimentation rates remain high throughout the Late Cretaceous.

Cyclostratigraphy could both test and calibrate estimates currently constrained by nannofossil events and so allow detailed and precise comparison of sedimentation rates through time. Specifically, if the NGR and MS variations are paced by astronomical cycles and sedimentation was relatively continuous, decreases in sedimentation rates should be apparent by a decrease in cycle thicknesses. However, accurate cyclostratigraphic interpretations will be difficult to generate if there were times of frequent non-deposition as may be the case for the Coniacian and younger intervals.

Site U1512 could also be a boon for studies of circulation in the early Southern Ocean. Several studies have shown that ε_{Nd} values varied widely among austral sites from the Cenomanian at least to the Campanian (Robinson et al., 2010; Murphy and Thomas, 2012, 2013; Moiroud et al., 2016). Regionally important water masses and local inputs of isotopically distinct Nd have both been invoked as explanations for this variation, but there is little control on the values for these potential sources. Measurements of ε_{Nd} values in detrital material from Site U1512 will provide a good control on likely inputs from the Australian continent while values from fish debris will connect that input to a water mass value that might be exported from the region as the rift deepened and became better connected to the southern Indian Ocean. Flow into the rift, on the other hand, would be suggested by dramatically different, likely higher, ε_{Nd} values in fish debris than is measured on the detrital fraction.

The scarcity of calcareous foraminifera will be a challenge for paleoclimatic work. Organic carbon contents are high enough (Fig. 6), though, that measurements of TEX_{86} values should be possible for much of the record providing constraints on evolution of regional surface

water temperatures. Along a similar line, analyses of inoceramid bivalves could augment or supplant benthic foraminiferal analyses as a means to estimate seafloor temperature trends.

Mineralogy of terrigenous material and biomarker studies might provide clues to climatic conditions in the terrestrial realm of southern and southeastern Australia. The excursion to lower NGR and MS values at ~330 mbsf in Hole U1512A (Fig. 7) coincides with a possible sequence boundary and an increase in both amorphous silica and kaolinite contents. The latter is considered to be a consequence of high degrees of chemical weathering (e.g., Thiry, 2000), a climatically sensitive process. On short timescales, the apparent cyclicity observed in the NGR and MS signals suggest an orbital control of terrestrial weathering and/or hydrology that influenced terrigenous input. Determining the cause of the change in physical properties (e.g., shifts in clay mineralogy, subtle grain-size variation) could constrain how weathering and sediment transport varied in a greenhouse world at >60°S latitude.

Finally, integrated findings for Site U1512 provide new insights into the structural evolution of the sub-basins within the Great Australian Bight. Prior to coring, there was no way to accurately tie seismic reflectors across the fault zone – despite the Jerboa-1 exploration well being drilled in the footwall of the fault system, ~12 km NNW from Site U1512 (Totterdell et al., 2000; Totterdell and Bradshaw, 2004). As Site U1512 was cored in the hanging wall block over the Wallaroo Fault Zone, we now know that there is a major difference in the thickness of the Turonian–Santonian sequences on either side of this fault (Fig. 1). This difference suggests that the Wallaroo Fault Zone was active during deposition in the Turonian–Santonian, with ongoing displacement accommodating the continual deposition of the sequences cored at Site U1512. The normal displacement along this fault zone is coincident with the timing of slow rifting/spreading between Australia and Antarctica. Also, while the Jerboa-1 well intersected a ~150 m-thick sequence of Eocene to Oligocene sediments above the Tiger Supersequence, these sequences were not recovered at Site U1512. We suspect these younger sequences were displaced as part of a slump located near to the coring site (Fig. 1).

Conclusion

Cores from Site U1512 extend down to 700 mbsf with excellent recovery (>90%) and good age control. The upper 10 m of sediment recovered is Pleistocene nannofossil and foraminiferal ooze that sits disconformably upon at least 690 m of black silty clays and claystones of early Campanian to early Turonian age, which correlates to the Tiger Supersequence defined from nearby well data and land-based sections (e.g., Totterdell et al., 2000). The sequence at Site U1512 is biostratigraphically complete and comprised of a remarkably uniform succession of terrigenous silty claystone with low to very low abundances of calcareous microfossils. Organic carbon content is less than 1.5% throughout, and the consistent presence of bioturbation through the Upper Cretaceous interval indicates that bottom waters were generally oxygenated. The relative stability of the depositional regime suggested by the limited lithologic variability should increase the signal to noise ratio in interpretation of geochemical proxies, but the scarcity of calcareous microfossils will necessitate integrated studies to understand paleoceanographic and paleoenvironmental conditions. Knowledge of trends in the depositional environment at Site U1512 will provide new constraints on the evolution of the deeper parts of the Ceduna Sub-basin between 93 and 83 Ma.

References

Amante, C., and Eakins, B. W., 2009, ETOPO1 1 Arc-Minute Global Relief Model: Procedures, Data Sources and Analysis. : NOAA Technical Memorandum NESDIS NGDC-24. National Geophysical Data Center, NOAA.

Anagnostou, E., John, E. H., Edgar, K. M., Foster, G. L., Ridgwell, A., Inglis, G. N., Pancost, R. D., Lunt, D. J., and Pearson, P. N., 2016, Changing atmospheric CO_2 concentration was the primary driver of early Cenozoic climate: Nature, v. 533, p. 380-384.

Bijl, P. K., Bendle, J. A., Bohaty, S. M., Pross, J., Schouten, S., Tauxe, L., Stickley, C. E., McKay, R. M., Röhl, U., and Olney, M., 2013, Eocene cooling linked to early flow across the Tasmanian Gateway: Proceedings of the National Academy of Sciences, v. 110, p. 9645-9650.

Boger, S. D., 2011, Antarctica-before and after Gondwana: Gondwana Research, v. 19, p. 335-371.

DeConto, R. M., and Pollard, D., 2003, Rapid Cenozoic glaciation of Antarctica induced by declining atmospheric CO_2: Nature, v. 421, p. 245-249.

Direen, N. G., Stagg, H. M. J., Symonds, P. A., and Colwell, J. B., 2011, Dominant symmetry of a conjugate southern Australian and East Antarctic magma-poor rifted margin segment: Geochemistry, Geophysics, Geosystems, v. 12, p. Q02006.

Elder, W. P., 1985, Biotic Patterns Across the Cenomanian-Turonian Extinction Boundary Near Pueblo, Colorado, *in* Pratt, L. M., Kauffman, E. G., and Zelt, F. B., eds., Fine-Grained Deposits and Biofacies of the Cretaceous Western Interior Seaway: Evidence of Cyclic Sedimentary Processes, Volume 4: Tulsa, OK, SEPM Society for Sedimentary Geology, p. 157-169.

Exon, N., Kennett, J. P., Malone, M. J., and Party, L. S., 2001, Leg 189 Summary, *in* Exon, N., Kennett, J. P., and Malone, M. J., eds., Proceedings of the Ocean Drilling Program, Initial Report, Volume 189: College Station, TX, p. 1-98.

Falzoni, F., Petrizzo, M.R., Clarke, L.J., MacLeod, K.G., and Jenkyns, H.C., 2016, Long-term Late Cretaceous carbon- and oxygen-isotope trends and planktonic foraminiferal turnover: a new record from the southern mid latitudes: Geological Society of America Bulletin, v. 128, p. 1725-1735, doi: 10.1130/B31399.1

Frey, F. A., Coffin, M. F., Wallace, P. J., Weis, D., Zhao, X., Wise, S. W., Wähnert, V., Teagle, D. A. H., Saccocia, P. J., Reusch, D. N., Pringle, M. S., Nicolaysen, K. E., Neal, C. R., Müller, R. D., Moore, C. L., Mahoney, J. J., Keszthelyi, L., Inokuchi, H., Duncan, R. A., Delius, H., Damuth, J. E., Damasceno, D., Coxall, H. K., Borre, M. K., Boehm, F., Barling, J., Arndt, N. T., and Antretter, M., 2000, Origin and evolution of a submarine large igneous province: the Kerguelen Plateau and Broken Ridge, southern Indian Ocean: Earth and Planetary Science Letters, v. 176, no. 1, p. 73-89.

Gallagher, S. J., Taylor, D., Apthorpe, M., Stilwell, J. D., Boreham, C. J., Holdgate, G. R., Wallace, M. W., and Quilty, P. G., 2005, Late Cretaceous dysoxia in a southern high latitude siliciclastic succession, the Otway Basin, southeastern Australia: Palaeogeography, Palaeoclimatology, Palaeoecology, v. 223, p. 317-348.

Gräfe, K.-U., Wendler, J., 2003. Foraminifers and calcareous dinoflagellate cysts as proxies for deciphering sequence stratigraphy, sea-level change, and paleoceanography of Cenomanian-Turonian hemipelagic sediments in Western Europe. In: Olsen, H.C., Leckie, R.M. (Eds.), Micropaleontologic Proxies for Sealevel Change and Stratigraphic Discontinuities, SEPM Special Publication 75, 229-262.

Hardenbol, J., Thierry, J., Farley, M. B., Jacquin, T., Graciansky, P.-C. d., and Vail, P. R., 1998, Mesozoic and Cenozoic Sequence Chronostratigraphic Framework of European Basins, *in* Graciansky, P.-C. d., Hardenbol, J., Jacquin, T., and Vail, P. R., eds., Volume 60, SEPM Society for Sedimentary Geology, p. 329-332.

Haynes, S.J., MacLeod, K.G., Ladant, J.-B., Vande Guchte, A., Asgharian R.M., Poulsen, C.J., and Martin, E.E., 2020, Constraining sources and relative flow rates of bottom waters in the Late Cretaceous Pacific Ocean: Geology, v. 48, in press.

Henderson, R. A., 2004, A Mid-Cretaceous Association of Shell Beds and Organic-rich Shale: Bivalve Exploitation of a Nutrient-Rich, Anoxic Sea-floor Environment: PALAIOS, v. 19, p. 156-169.

Holbourn, A.E.L., and Moullade, M., 1998. Lower Cretaceous benthic foraminifer assemblages, equatorial Atlantic: biostratigraphic, paleoenvironmental, and paleobiogeographic significance, *in* Mascle, J., Lohmann, G.P., and Moullade, M. (eds.), Proceedings of the Ocean Drilling Program, Scientific Results, Volume 159: College Station, TX (Ocean Drilling Program), p. 347–362. doi:10.2973/odp.proc.sr.159.033.1998

Huber, B. T., Hobbs, R. W., Bogus, K. A., Batenburg, S. J., Brumsack, H.-J., doMonteGuerra, R., Edgar, K. M., Edvardsen, T., Harry, D. L., Hasegawa, T., Haynes, S. J., Jiang, T., Jones, M.M., Kuroda, J., Lee, E. Y., Li, Y.-X., MacLeod, K. G., Maritati, A., Martinez, M., O'Connor, L. K., Petrizzo, M. R., Quan, T. M., Richter, C., Riquier, L., Tagliaro, G. T., Garcia Tejada, M. L., Wainman, C. C., Watkins, D. K., White, L. T., Wolfgring, E., and Xu, Z., 2019, Site U1512, *in* Hobbs, R. W., Huber, B. T., Bogus, K. A., and Expedition Scientists, eds., Proceedings of the International Ocean Discovery Program, Initial Reports, Volume 369: College Station, TX (International Ocean Discovery Program), p. 1-30.

Huber, B. T., MacLeod, K. G., Watkins, D. K., and Coffin, M. F., 2018, The rise and fall of the Cretaceous hot greenhouse climate: Global and Planetary Change, v. 167, p. 1-23.

Huber, B. T., Norris, R. D., and MacLeod, K. G., 2002, Deep-sea paleotemperature record of extreme warmth during the Cretaceous: Geology, v. 30, no. 2, p. 123-126.

Huber, B.T., Hodell, D.A., and Hamilton, C.P., 1995, Mid- to Late Cretaceous climate of the southern high latitudes: Stable isotopic evidence for minimal equator-to-pole thermal

gradients: Geological Society of America Bulletin, v. 107, p. 1164-1191.

Huck, C. E., van de Flierdt, T., Bohaty, S. M., and Hammond, S. J., 2017, Antarctic climate, Southern Ocean circulation patterns, and deep water formation during the Eocene, Paleoceanography: 10.1002/2017PA003135, v. 32, no. 7, p. 674-691.

Hunt, C., Moskowitz, B. M., and Banerjee, S. K., 1995, Magnetic Properties of Rocks and Minerals, *in* J., A. T., ed., Rock Physics and Phase Relations: A Handbook of Physical Constants: Washington D.C., USA, American Geophysical Union, p. 189-204.

Jiménez Berrocoso, Á., MacLeod, K. G., Calvert, S. E., and Elorza, J., 2008, Bottom water anoxia, inoceramid colonization, and benthopelagic coupling during black shale deposition on Demerara Rise (Late Cretaceous western tropical North Atlantic): Paleoceanography, v. 23, no. 3, p. 1-20.

Jordan, T. E., 1981, Thrust loads and foreland basin evolution, Cretaceous, western United States: American Association of Petroleum Geologists Bulletin, v. 65, p. 2506-2520.

Kaminski, M.A., Gradstein, F.M., 2005. Atlas of Paleogene Cosmopolitan Deep–Water Agglutinated Foraminifera, Grzybowski Foundation Special Publication, v. 10. Kraków, 547 pp.

Kauffman, E. G., Harries, P. J., Meyer, C., Villamil, T., Arango, C., and Jaecks, G., 2007, Paleoecology of giant inoceramidae (Platyceramus) on a Santonian (Cretaceous) seafloor in Colorado: Journal of Paleontology, v. 81, no. 1, p. 64-81.

Kennett, J. P., 1977, Cenozoic evolution of Antarctic glaciation, the Circum-Antarctic Ocean, and their impact on global paleoceanography: Journal of Geophysical Research, v. 82, p. 3843-3860.

Kita, Z. A., Watkins, D. K., and Sageman, B. B., 2017, High-resolution calcareous nannofossil biostratigraphy of the Santonian/Campanian Stage boundary, Western Interior Basin, USA.: Cretaceous Research, v. 69, p. 49-55.

Leckie, R.M., Yuretich, R.F., West, O.L.O., Finkelstein, D., and Scmidt, M., 1998, Paleoceanography of the Southwestern Western Interior Sea During the Time of the Cenomanian-Turonian Boundary (Late Cretaceous) *in* Dean, W.E., and Arthur, M.A., eds., Stratigraphy and Paleoenvironments of the Cretaceous Western Interior Seaway, USA: SEPM, Concepts in Sedimentology and Paleontology, no. 6, p.101–126, doi: org/10.2110/csp.98.06.0101.

Locklair, R. E., and Sageman, B. B., 2008, Cyclostratigraphy of the Upper Cretaceous Niobrara Formation, Western Interior, U.S.A.: A Coniacian–Santonian orbital timescale: Earth and Planetary Science Letters, v. 269, no. 3-4, p. 540-553.

Lowery, C. M., Leckie, R. M., and Sageman, B. B., 2017, Micropaleontological evidence for redox changes in the OAE3 interval of the US Western Interior: Global vs local processes: Cretaceous Research, v. 69, p. 34-48.

MacDonald, J. D., Holford, S. P., Green, P. F., Duddy, I. R., King, R. C., and Backé, G., 2013, Detrital zircon data reveal the origin of Australia's largest delta system: Journal of the Geological Society, v. 170, p. 3-6.

MacLeod, K. G., 1994, Bioturbation, inoceramid extinction, and mid-Maastrichtian ecological change: Geology, v. 22, no. 2, p. 139-142.

MacLeod, K. G., and Hoppe, K. A., 1992, Evidence that inoceramid bivalves were benthic and harbored chemosynthetic symbionts: Geology, v. 20, p. 117-120.

MacLeod, K. G., and Huber, B. T., 2001, The Maastrichtian record at Blake Nose (western North Atlantic) and implications for global palaeoceanographic and biotic changes, *in* Kroon, R., Norris, R. D., and Klaus, A., eds., Western North Atlantic Palaeogene and Cretaceous Palaeoceanography, Volume 183: London, Geological Society, p. 111-130.

MacLeod, K. G., Huber, B. T., and Ward, P. D., 1996, "The biostratigraphy and paleobiogeography of Maastrichtian inoceramids", *in* Ryder, G., CGartner, S., and Fastovsky, D., eds., New Developments Regarding the KT Event and Other Catastrophes in Earth History, Geological Society of America Special Papers, Volume 307: Boulder, Geological Society of America, p. 361-371.

MacLeod, K. G., and Irving, A. J., 1996, Correlation of cerium anomalies with indicators of paleoenvironment: Journal of Sedimentary Research, v. 66, no. 5, p. 948-955.

Meyers, S. R., 2012, Seeing red in cyclic stratigraphy: Spectral noise estimation for astrochronology: Paleoceanography, v. 27, p. PA3228.

Moiroud, M., Pucéat, E., Donnadieu, Y., Bayon, G., Guiraud, M., Voigt, S., Deconinck, J. F., and Monna, F., 2016, Evolution of neodymium isotopic signature of seawater during the Late Cretaceous: Implications for intermediate and deep circulation: Gondwana Research, v. 36, p. 503-522.

Murphy, D. P., and Thomas, D. J., 2012, Cretaceous deep-water formation in the Indian sector of the Southern Ocean: Paleoceanography, v. 27, no. 1, p. PA1211.

-, 2013, The evolution of Late Cretaceous deep-ocean circulation in the Atlantic basins: Neodymium isotope evidence from South Atlantic drill sites for tectonic controls: Geochemistry, Geophysics, Geosystems, v. 14, no. 12, p. 5323-5340.

Norvick, M. S., and Smith, M. A., 2001, Mapping the plate tectonic reconstruction of southern and southeastern Australia and implications for petroleum systems: The APPEA Journal, v. 41, p. 15-35.

O'Connor, L., Robinson, S., Naafs, B. D., Jenkyns, H., Henson, S., Clarke, M., and Pancost, R., 2019, ate Cretaceous Temperature Evolution of the Southern High Latitudes: A TEX86 Perspective: Paleoceanography and Paleoclimatology, v. 34, p. 1-19.

Pang, M., and Nummedal, D., 1995, Flexural subsidence and basement tectonics of the Cretaceous Western Interior basin, United States: Geology, v. 23, p. 173-176.

Perch-Nielsen, K., 1985, Mesozoic calcareous nannofossils, *in* Bolli, H. M., Saunders, J. B., and Perch-Neilsen, K., eds., Plankton Stratigraphy: Cambridge, Cambridge University Press, p. 329-426.

Pimmel, A., and Claypool, G., 2001, Introduction to Ship- board Organic Geochemistry on the JOIDES Resolution: Technical Note Ocean Drilling Program, v. 30, p. 1-20.

Quirein, J. A., Gardner, J. S., and Watson, J. T., 1982, Combined Natural Gamma-Ray Spectral/Litho-density Measurements Applied to Clay Mineral Identification: Bulletin-American Association of Petroleum Geologists, v. 66, no. 9, p. 1446-1446.

Robinson, S. A., Murphy, D. P., Vance, D., and Thomas, D. J., 2010, Formation of "Southern Component Water" in the Late Cretaceous: Evidence from Nd-isotopes: Geology, v. 38, no. 10, p. 871-874.

Royer, J. Y., and Rollet, N., 1997, Plate-tectonic setting of the Tasmanian region: Australian Journal of Earth Sciences, v. 44, no. 5, p. 543-560.

Sageman, B. B., 1989, The benthic boundary biofacies model: Hartland Shale Member, Greenhorn Formation (Cenomanian), Western Interior, North America: Palaeogeography, Palaeoclimatology, Palaeoecology, v. 74, no. 1-2, p. 87-110.

Sageman, B. B., and Bina, C. R., 1997, Diversity and species abundance patterns in Late Cenomanian black shale biofacies, Western Interior, US: Palaios, v. 5, p. 449-466.

Sageman, B. B., Rich, J., Arthur, M. A., Birchfield, G. E., and Dean, W. E., 1997, Evidence for Milankovitch periodicities in Cenomanian-Turonian lithologic and geochemical cycles, western interior USA: Journal of Sedimentary Research, v. 2, p. 286-302.

Savrda, C. E., and Bottjer, D. J., 1989, Trace-fossil model for reconstructing oxygenation histories of ancient marine bottom waters: Application to Upper Cretaceous Niobrara Formation, Colorado: Palaeogeography, Palaeoclimatology, Palaeoecology, v. 74, no. 1-2, p. 49-74.

Sayers, J., Symonds, P., Direen, N., and Bernardel, G., 2001, Nature of the continent-ocean transition on the non-volcanic rifted margin of the central Great Australian Bight: Geological Society of London Special Publication, v. 187, p. 51-76.

Scher, H. D., Whittaker, J. M., Williams, S. E., Latimer, J. C., Kordesch, W. E. C., and Delaney, M. L., 2015, Onset of Antarctic circumpolar current 30 million years ago as Tasmanian gateway aligned with westerlies: Nature, v. 523, p. 580-583.

Smith, J. W., and Pallasser, R. J., 1996, Microbial origin of Australian coalbed methane: American Association of Petroleum Geologists Bulletin, v. 80, p. 891-897.

Stagg, H. M. J., Cockshell, C. D., Willcox, J. B., Hill, A. J., Needham, D. J. L., Thomas, B., O'Brien, G. W., and Hough, L. P., 1990, Basins of the Great Australian Bight Region. Geology and Petroleum Potential, Bureau of Mineral Resources Australia.

Strąpoć, D., Mastalerz, M., Schimmelmann, A., Drobniak, A., and Hedges, S., 2008, Variability of geochemical properties in a microbially dominated coalbed gas system from the eastern margin of the Illinois Basin, USA: International Journal of Coal Geology, v. 76, p. 98-110.

Tjalsma, R. C.; Lohmann, G. P., 1983. Paleocene-Eocene bathyal and abyssal benthic foraminifera from the Atlantic Ocean: Micropaleontology, Special Publication, v. 4, p. 1-90.

Thiry, M., 2000, Palaeoclimatic interpretation of clay minerals in marine deposits: An outlook from the continental origin: Earth Science Reviews, v. 49, p. 201-221.

Tikku, A. A., and Direen, N. G., 2008, Comment on "Major Australian-Antarctic plate reorganization at Hawaiian emperor bend time": Science, v. 321, p. 490.

Torres, M. E., Brumsackb, H. J., Bohrmann, G., and Emeis, K. C., 1996, Barite fronts in continental margin sediments: a new look at barium remobilization in the zone of sulfate reduction and formation of heavy barites in diagenetic fronts: Chemical Geology, v. 127, p. 125-139.

Totterdell, J. M., Blevin, J. E., Struckmeyer, H. I. M., Bradshaw, B. E., Colwell, J. B., and Kennard, J. M., 2000, A new sequence framework for the Great Australian Bight starting with a clean slate: The APPEA Journal v. 2000, p. 95-117.

Totterdell, J. M., and Bradshaw, B. E., 2004, The structural framework and tectonic evolution of the Bight Basin, *in* Boult, P. J., Johns, D. R., and Lang, S. C., eds., PESA's Eastern Australian Basins Symposium II p. 41-61.

Totterdell, J. M., and Mitchell, C., 2009, Bight Basin geological sampling and seepage survey: R/V Southern Surveyor Survey SS01/2007, v. Geoscience Australia, Record, 2009/24, 134 p.

van den Ende, C., White, L. T., and van Welzen, P. C., 2017, The existence and break-up of the Antarctic land bridge as indicated by both amphi-Pacific distributions and tectonics: Gondwana Research, v. 44, p. 219-227.

van Hinsbergen, D. J., de Groot, L. V., van Schaik, S. J., Spakman, W., Bijl, P. K., Sluijs, A., Langereis, C. G., and Brinkhuis, H., 2015, A paleolatitude calculator for paleoclimate studies: PLoS ONE, v. 10, p. p.e0126946.

Van Morkhoven, F.P.C.M., Berggren, W.A. and Edwards, A.S., 1986. Cenozoic cosmopolitan deep-water benthic foraminifera. Bullettin Centres Recherches Exploration-Prodroduction Elf-Aquitaine Mémoire, v. 11, 421 pp.

Veevers, J. J., 2012, Reconstructions before rifting and drifting reveal the geological connections between Antarctica and its conjugates in Gondwanaland: Earth-Science Reviews, v. 111, p. 249-318.

Watkins, D. K., Bralower, T. J., Covington, J. M., and Fisher, C. G., 1993, Biostratigraphy and paleoecology of the Upper Cretaceous calcareous nannofossil in the Western Interior Basin, North America, *in* Caldwell, W. G. E., and Kauffman, E. G., eds., Cretaceous Evolution of the Western Interior Basin of North America, Special Paper 39, Geolological Association of Canada, p. 521-537.

Watkins, D.K., S.W. Wise, Jr., J.J. Pospichal, and J. Crux, 1996, Upper Cretaceous calcareous nannofossil biostratigraphy and paleoceanography of the Southern Ocean, *in* Moguilevsky, A. and Whatley, R.C., eds., Microfossils and Oceanic Environments; British Micropalaeontological Society, University of Wales, Aberystwyth Press, p. 355-381.

White, L. T., Gibson, G. M., and Lister, G. S., 2013, A reassessment of paleogeographic reconstructions of eastern Gondwana: bringing geology back into the equation: Gondwana Research, v. 24, p. 984-998.

Whiticar, M. J., 1994, Correlation of natural gases with their sources, *in* Magoon, L. B., and Dow, W. G., eds., The petroleum system—from source to trap, AAPG Memoir Volume 60, AAPG, p. 261-283.

Willcox, J. B., and Stagg, H. M. J., 1990, Australia's southern margin: a product of oblique extension: Tectonophysics, v. 173, no. 1-4, p. 269-281.

Figure Captions:

Figure 1- Upper panel- position of IODP Site U1512 within the NW portion of the Ceduna Sub-basin in the Great Australian Bight (area shown indicated by box inset map). Also shown are nearby commercial wells (open circles) from which logging data and cuttings were used to define regional stratigraphic units (Totterdell et al., 2000) and sites cored during Ocean Drilling Program Leg 182 (small gray circles), none of which cored and/or drilled deep enough to penetrate Cretaceous sediments. Lower panel- interpreted and annotated seismic reflection profile along line A-A´ (AGSO S065_06) that links IODP Site U1512 with the nearby Jerboa-1 well. Stratigraphic nomenclature from Totterdell et al. (2000).

Figure 2- Tectonic reconstruction of the Australo-Antarctica Gulf at 90 Ma showing the approximate position of the coastlines at this time (the green +200 m contour). The image was produced by rotating the plate fragments using the poles of rotation provided by van den Ende et al. (2017) with the modern-day bathymetry/topography (ETOPO 1 Bedrock dataset: Amante and Eakins (2009). The ETOPO1 Bedrock grid estimates the Earth's topography by subtracting best estimates of ice thickness derived from geophysical measurements. This image assumes global-sea level was ~200 m higher than the present day and that there has been no change in the Earth's topography since 90 Ma; it does not account for isostacy associated with the subtraction of ice cover from Antarctica, so the Antarctic land surface would likely be greater than is implied here. Because modern continental topography is used, the reconstruction shows the Tasman Gateway as less restricted than it was during the Late Cretaceous.

Figure 3- Graphic representation of selected sedimentological and paleontological summary observations in IODP Hole U1512A (after Huber et al., 2019). Recovery (shown by black fill) was excellent throughout the Cretaceous. Cretaceous rocks are quite uniform and are dominantly dark silty claystones and clayey siltstones. Age is best constrained by calcareous nannofossil biostratigraphy. On the age-depth plot, events plotted are top *Eprolithus floralis,* base *Calculites obscurans* (BCo), top *Lithostrinus septenarius* (TLs), base *Reinhardtites anthophorus* (BRa), base *Micula staurophora* (BMs), base *Marthasterites furcatus* (BMf), base *Eiffelithus eximius* [sensu Verbeek] (BEe), base *Quadrum gartneri* (BQg), and base *Eprolithus moratus* (BEm). Note the latter event is a minimum depth as it occurs at the bottom of the hole and implied sedimentation rate is thus shown with a dashed line. Planktonic foraminiferal biostratigraphy and magnetostratigraphy (Huber et al., 2019) provide similar age estimates but lower resolution.

Average sediment accumulation rates are given in meters per million years. Lithologic Unit I is calcareous ooze. In the Magnetostratigraphy column, black represents normal polarity, white reversed polarity, and gray uncertain polarity. Calcareous microfossils are generally rare but commonly present. The presence of these groups as well as selected other fossils at a core-level resolution are shown by gray shading in the respective columns. Calcareous fossils are effectively absent from 200 to 300 m below seafloor (benthic foraminifera in this interval are agglutinated taxa). Large dinoflagellate cysts are more common low in the section whereas radiolaria are more common higher in the section.

Figure 4- Photographs typical of the major (A-D) and minor (E, F) lithologies recovered in IODP Hole U1512A. A, B) massive to faintly burrow mottled textures. C, D) distinctly mottled textures with discrete burrows. E) siderite cemented sideritic sandstone grading upwards to silty claystone. F) glauconitic sandstone with a claystone intraclast. All photo are 7 cm wide.

Figure 5- Inoceramid bivalves in U1512 cores. A) An individual inoceramid showing borings from epibionts on shell surface (examples circled) as well as scattered shell fragments from other individuals (black arrows) on the bedding surface at U1512A-67R-CC, 0 cm, 641.42 mbsf. B) Cross-section of an inoceramid shell at U1512A-8R-6, 46–52 cm, 74.91 mbsf. Individual prismatic shell fragments (white arrows) scattered on cut surface on surface of split core demonstrate lack of cementation of this shell.

Figure 6: Headspace methane:ethane ratios, bulk sediment carbonate content (CaCO3), bulk sediment total organic carbon (TOC), and bulk sediment TOC: total nitrogen (TN) ratio. The high methane:ethane ratios between ~300-450 mbsf indicate the presence of bacterial methanogenesis.

Figure 7- Long and short-scale variations in the magnetic susceptibility (MS) and Natural Gamma Ray (NGR) signals plotted against depth in Hole U1512A. A) MS signal (in orange) with long-scale trend (in black) calculated using a LOWESS (Locally Weighted Scatterplot Smoothing) curve with a coefficient of 20%. IU: Instrument Unit (Cleveland, 1979). B) NGR signal (in red) with the long-scale trend (in black) obtained as in panel A. cps: counts per second. The horizontal blue band represents an excursion to lower MS and NGR values. C) Details of the NGR signal from 105 to 180 mbsf (in grey) with filter of the cycles from 3 to 5 m (orange). To extract the 3-to-5-m cycles, a Taner bandpass filter was applied to the NGR series with a low

cutoff frequency of 0.05376 cycles/m, a high cutoff frequency of 0.3659 cycles/m and a roll-off rate of 10^{36}. D) Spectrum of the NGR signal from 105 to 180 mbsf, showing two cycles at 5.5 and 3.9 m. The confidence levels reveal the significance of the cycles against a model of red noise (see Meyers, 2012). E) Spectrogram (3-dimension spectrum) applied on 20-m-long window revealing the evolution of the cycles throughout the studied interval. One period is observed in red evolving from 3.2 to 5.6 m, suggesting that the two spectral peaks observed in panel D have the same origin. Their difference in period is simply due to variations in the sedimentation rate.

Figure 8. Five of the wireline logs recorded in borehole U1512A) natural gamma radiation which is consistent with the claystone/shale lithologies sampled from the recovered core. B) density which remains constant for the until about 270 m depth and then shows an increase with occasional high-density spikes that correlate to thin sideritic or glauconitic sand beds. C) p-wave velocity shows a general increase with depth. C) s-wave velocities show a similar increasing trend in the upper section but there is a significant decrease between 410 and 575 m depth which coincides with the interval of highest gamma measurement (>75 API); the separation of the two s-wave velocity measurements towards the base of the hole is probably due to the deviation of the hole from vertical. E) Deviation from vertical of the borehole starts at about 210 m depth and reaches a maximum of 26° at 650 m depth.

Author bios:

K.G. MacLeod is a professor at the University of Missouri, USA, who studies greenhouse paleoclimate and paleoceanography with an emphasis on the Late Cretaceous and mass extinctions. He sailed as a stratigraphic correlator on IODP Expedition 369.

L.T. White is a lecturer in geology at the University of Wollongong, Australia, whose principal research interest is the tectonic and paleogeographic history of Gondwana. Lloyd sailed on Expedition 369 as part of the physical properties and downhole logging team.

C.C. Wainman is a postdoctoral fellow at the University of Adelaide, Australia, who studies sedimentology, stratigraphy, and palynology. Carmine sailed on Expedition 369 as a sedimentologist and is investigating the evolution of Upper Cretaceous strata in the Bight Basin on Australia's southern margin.

M. Martinez is an assistant professor in sedimentology at the University of Rennes, France. His research interests focus on orbital forcing in the sedimentary record, reconstructing past climate changes, and building the geologic time scale. He sailed as a physical properties specialist on Expedition 369.

M.M. Jones is a postdoctoral fellow at the University of Michigan, USA, who researches Cretaceous paleoceanography and paleoclimatology using sedimentary geochemical analyses and quantitative stratigraphic techniques. He sailed on Expedition 369 as a downhole logging and physical properties specialist.

S.J. Batenburg is a research fellow at Géosciences Rennes, France, who studies paleoceanography and orbital forcing. She sailed on Expedition 369 as a stratigraphic correlator.

L. Riquier is an assistant professor in sedimentology and geochemistry at Sorbonne Université, France, who works on the environmental perturbations linked to oceanic anoxic events. He sailed on Expedition 369 as a sedimentologist. His research aims to better constrain the climatic and oceanographic conditions in the southwestern Australian margins during the Cenomanian-Turonian (100-90 Ma).

S.J. Haynes is a Research Specialist at Princeton University who studies paleoceanography. Shannon sailed as a sedimentologist on IODP Expedition 369 and her work focused on the use of neodymium isotopes from fossilized fish debris to better understand regional circulation in the Southern Ocean during the Late Cretaceous.

D.K. Watkins is the T.M Stout Distinguished Professor of Paleontology at the University of Nebraska, USA, who studies marine geology and micropaleontology. David sailed as a nannofossil specialist on Expedition 369 whose interests focused on the biostratigraphy and paleoceanography of the calcareous nannofossils from the Great Australian Bight and Naturaliste Plateau.
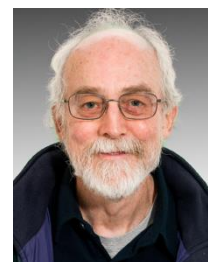
K.A. Bogus is the IODP-JRSO expedition project manager for Expedition 369. She is currently an honorary research fellow at the University of Exeter, UK. Her research interests include palynology and organic geochemistry.

H.-J. Brumsack is a professor emeritus at the University of Oldenburg, Germany. He sailed on Expedition 369 as an inorganic geochemist.

R. do Monte Guerra is a researcher at Unisinos University in south Brazil. His expertise is in micropaleontology and he sailed on Exp. 369 as a calcareous nannofossil specialist.

K.M. Edgar is a senior lecturer in micropalaeontology at the University of Birmingham, UK, who specializes in planktonic foraminifera and foraminifer-based geochemical

records to constrain interactions among global climate, geochemical cycling, and biota during the Cenozoic. Kirsty sailed on Expedition 369 as a planktic foraminifer micropaleontologist focusing on Paleogene paleoceanography.

T. Edvardsen is a postdoctoral researcher at the University of Exeter, UK, who studies benthic foraminiferal assemblages and isotopes. Trine sailed on Expedition 369 as a benthic foraminiferal specialist with a primary interest in reconstruction of paleoenvironments, productivity, and bathymetry proxies.

M.L. Garcia Tejada is a scientist at the Institute for Marine Geodynamics, Japan Agency for Marine-Earth Science and Technology who studies Large Igneous Provinces and their environmental effects. Maria Luisa sailed as a petrologist focusing on East Gondwana breakup and possible connections to later volcanism that formed the Kerguelen Plateau.

D.L. Harry is the Warner Professor of Geophysics at Colorado State University, USA, and studies the geodynamics of continental rifting. Dennis sailed as a physical properties specialist on Expedition 369 with interest in the processes that occurred during breakup and post-rift subsidence on the Australian margins.

T. Hasegawa is a Research Professor at Kanazawa University, Japan, who studies greenhouse paleoenvironments. Takashi sailed on Expedition 369 as an organic geochemist primarily interested in oceanic anoxic events, especially OAE2.

R.W. Hobbs is a professor at Durham University, UK, whose principal research area is marine geophysics. He sailed on Expedition 369 as a co-chief scientist.

B.T. Huber is a research geologist at the Smithsonian Institution, USA, whose research interests include the climate and oceanography of the Cretaceous Period and the extinction dynamics and evolution of planktonic foraminifera. He was a co-chief scientist during Expedition 369.

T. Jiang is a professor at the College of Marine Science and Technology, China University of Geosciences in Wuhan, China. His principal research interests focus on marine and petroleum geology. He sailed on Expedition 369 as a sedimentologist.

J. Kuroda is an associate professor at the Atmosphere and Ocean Research Institute, University of Tokyo, Japan, who studies paleoceanography. Kuroda sailed on Expedition 369 as a sedimentologist and will study temporal/secular changes in seawater osmium isotopic compositions through the Late Cretaceous to Cenozoic.

E.Y. Lee is a research fellow of basin analysis at Chonnam National University, South Korea. Her research focuses on quantitative basin analysis and visualization of sedimentary basins in Austria, western Australia and Korea. She was a shipboard scientist on Expedition 369 in the physical properties laboratory.

Y.-X. Li is a professor at Nanjing University, China, who studies paleomagnetism and paleoclimatology. Yong-Xiang sailed on Expedition 369 as a paleomagnetist.

A. Maritati is a PhD candidate at the Institute for Marine and Antarctic Studies, University of Tasmania, Australia, whose research focuses on the continental evolution of East Antarctica. He sailed on Expedition 369 as a sedimentologist with the aim of improving tectonic and paleogeographic reconstructions between India, Antarctica and Australia during Gondwana dispersal.
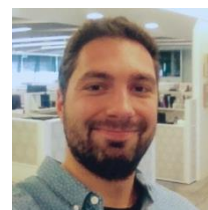
L.K. O'Connor is a postdoctoral researcher at the University of Arizona, USA, who uses organic geochemistry to reconstruct Cretaceous climate. Lauren is interested in the temperature evolution of the Cretaceous southern high latitudes and how climatic processes in this region responded to orbital forcing during periods of major climate change.

M.R. Petrizzo is Associate Professor in Paleontology and Paleoecology at the University of Milan, Italy, who studies Cretaceous and Cenozoic planktonic foraminifera. Maria Rose sailed on Expedition 369 as planktonic foraminifera micropaleontologist focusing on biostratigraphy, evolution, isotope paleoecology and paleoceanography of Cretaceous planktonic foraminifera.

T.M. Quan is an associate professor at Boone Pickens School of Geology, Oklahoma State University, USA, who studies the geochemistry of carbon and nitrogen in order to characterize paleoenvironmental conditions. Tracy sailed as a geochemist to investigate paleoredox conditions in the Paleogene and Cretaceous in relation to Southern Hemisphere climate and tectonic changes.

C. Richter is a professor and associate Dean at the University of Louisiana at Lafayette, USA, who studies paleomagnetism and rock magnetism. He sailed on Expedition 369 as a paleomagnetist.

G. Tagliaro is a PhD Candidate at the University of Texas at Austin, USA, who studies marine geology. He sailed on Expedition 369 as a sedimentologist.
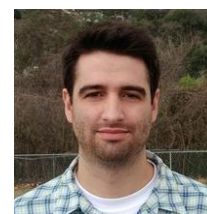
E. Wolfgring is a postdoctoral researcher at the University of Vienna, Austria, who is interested in paleoceanography and benthic foraminifera. Erik's primary interest during Expedition 369 was the Cretaceous benthic foraminiferal record.

Z. Xu is a professor at Institute of Oceanology, Chinese Academy of Sciences who studies paleoceanography and paleoclimate. Zhaokai focused on characteristics, forcing mechanisms, and global carbon cycle implications of the Oceanic Anoxic Events during the IODP Expedition 369.

Highlights
• Site 1512 provides 10 million year long record of pre-Southern ocean sedimentation.
• Interval recovered spans peak warmth during Late Cretaceous greenhouse.
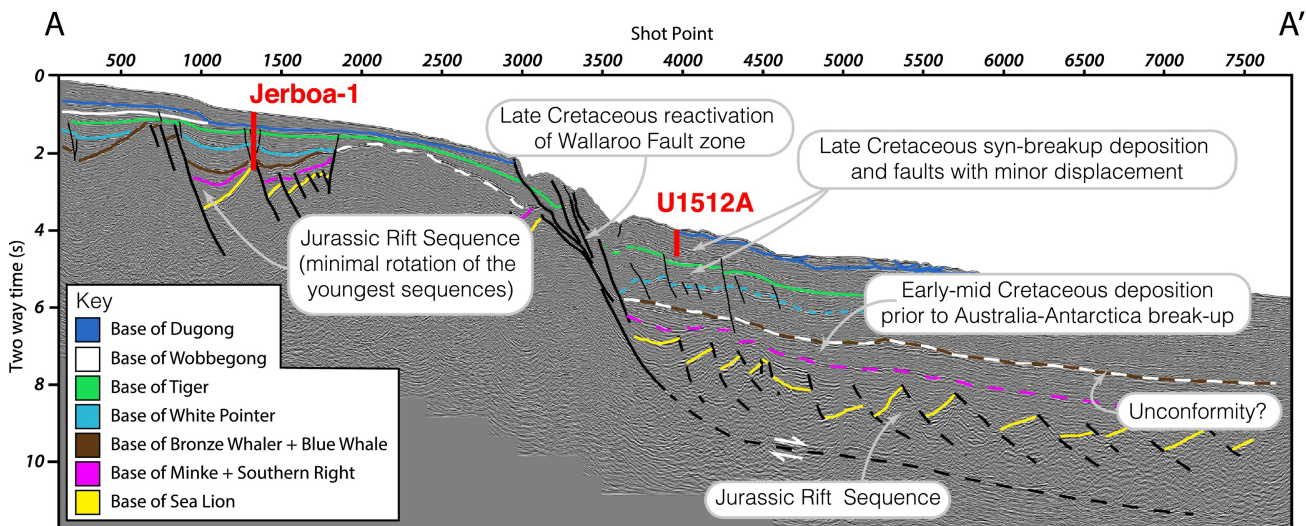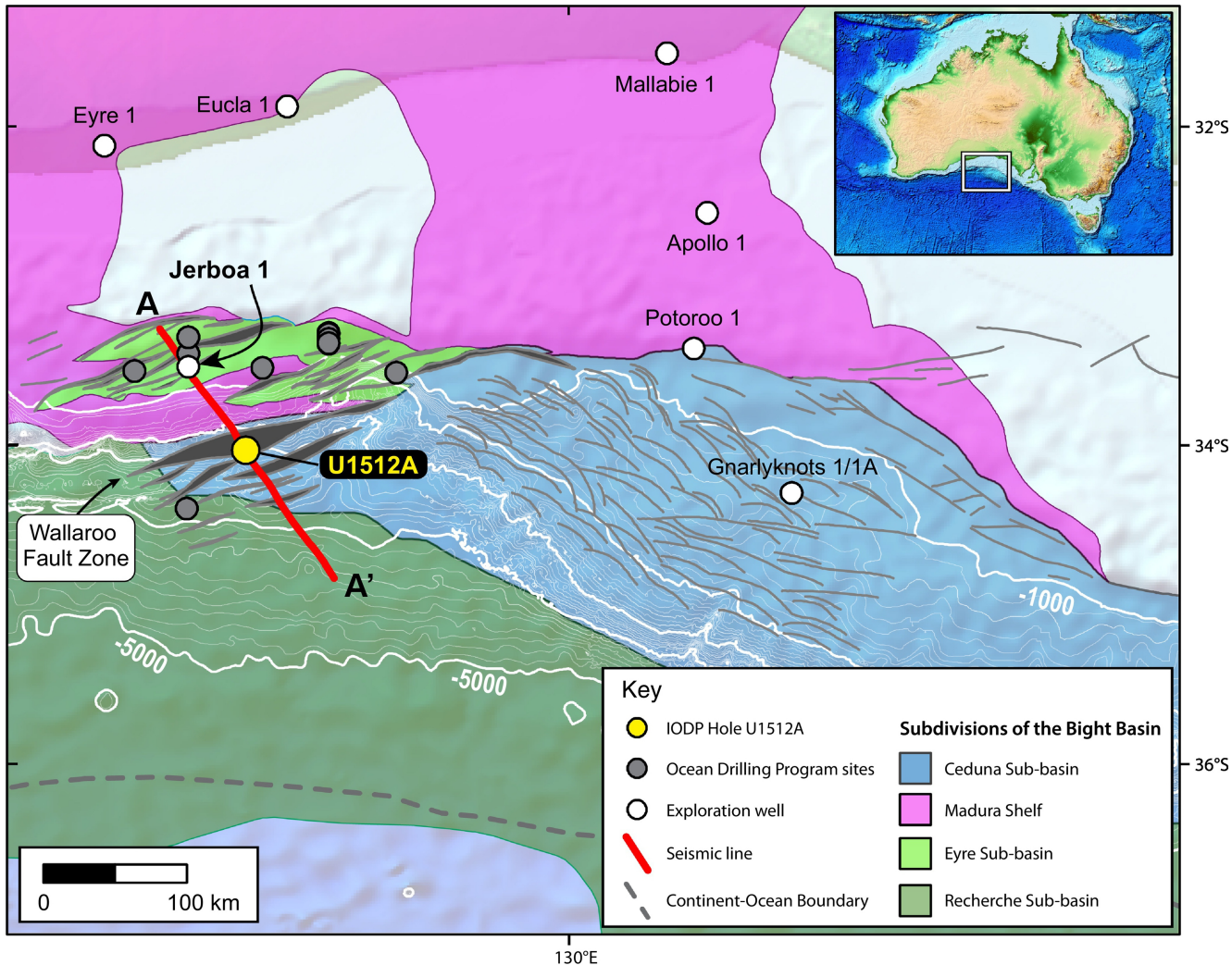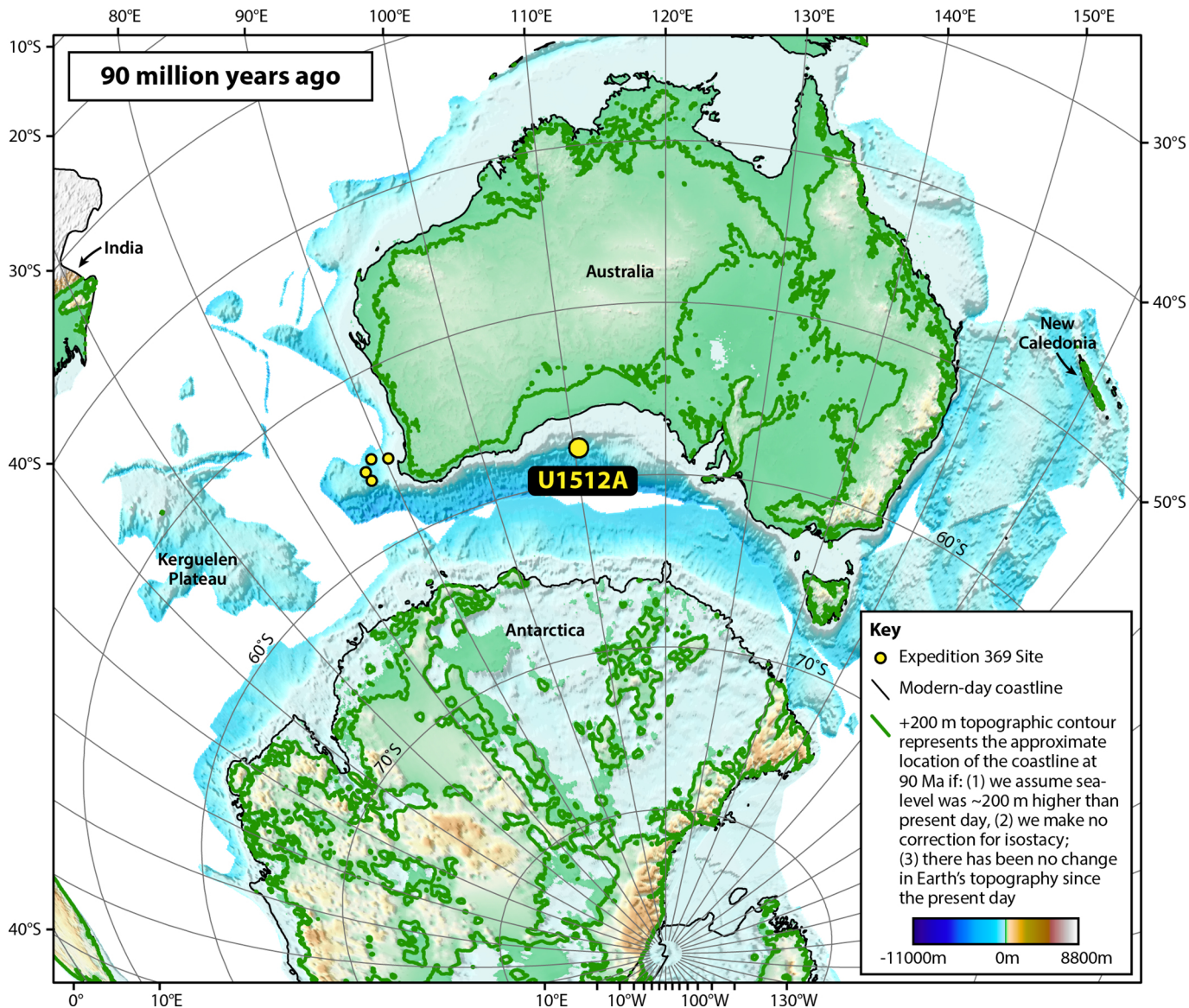• Paleoceanographic evolution illuminates relationships between climate and tectonics.

Figure 1
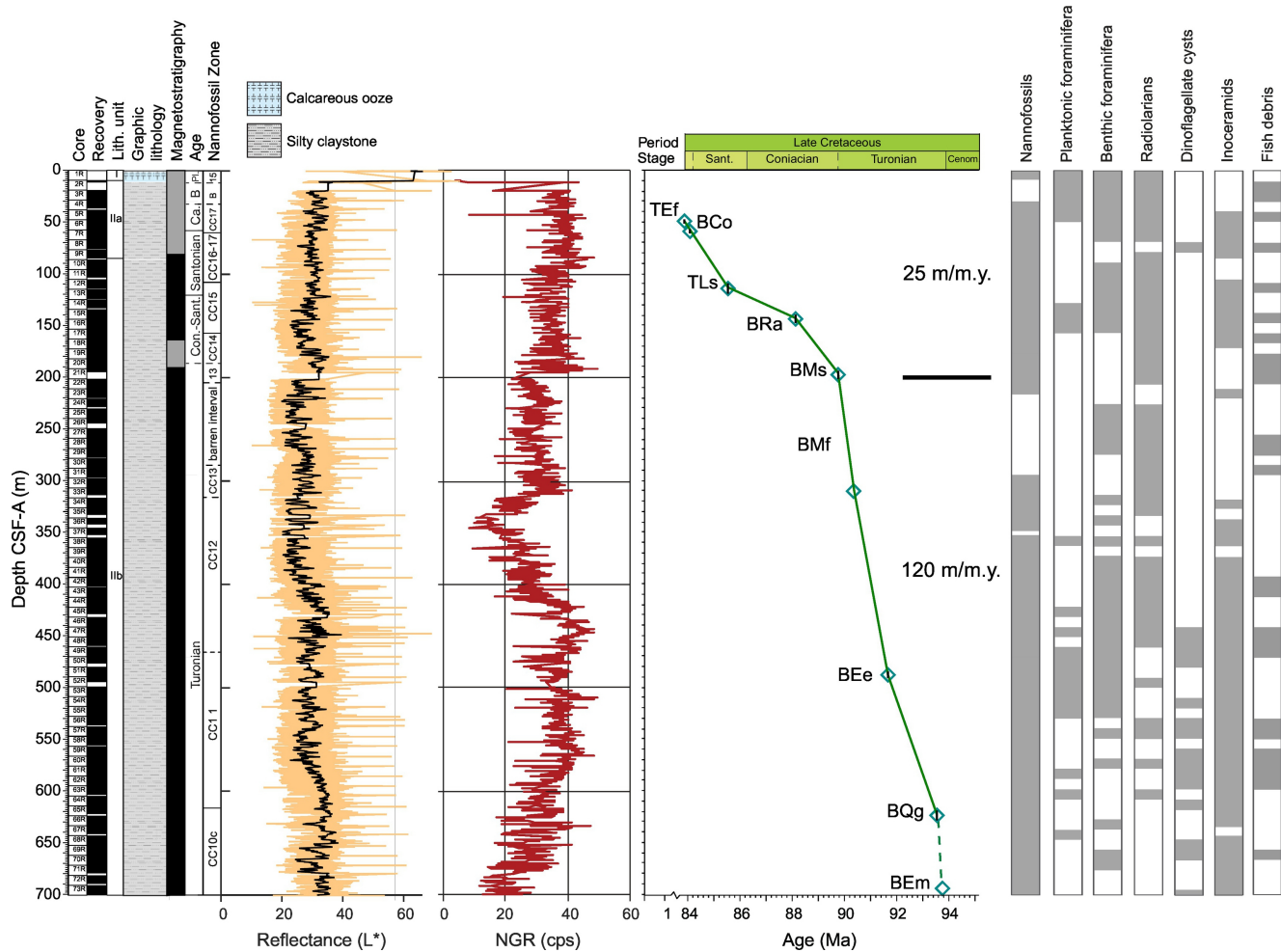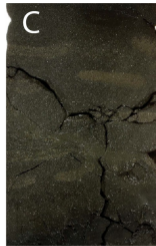
Figure 2

Figure 3

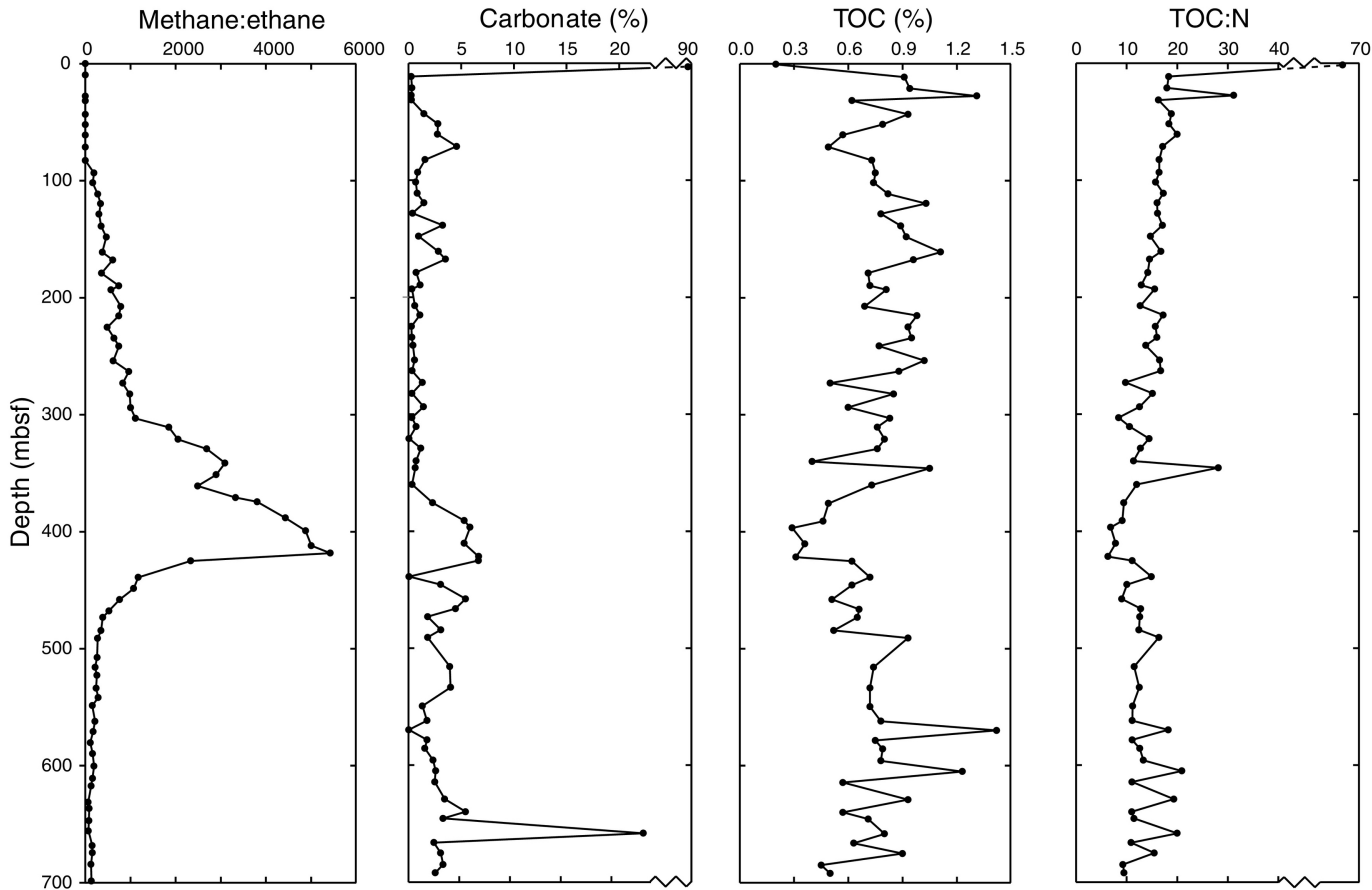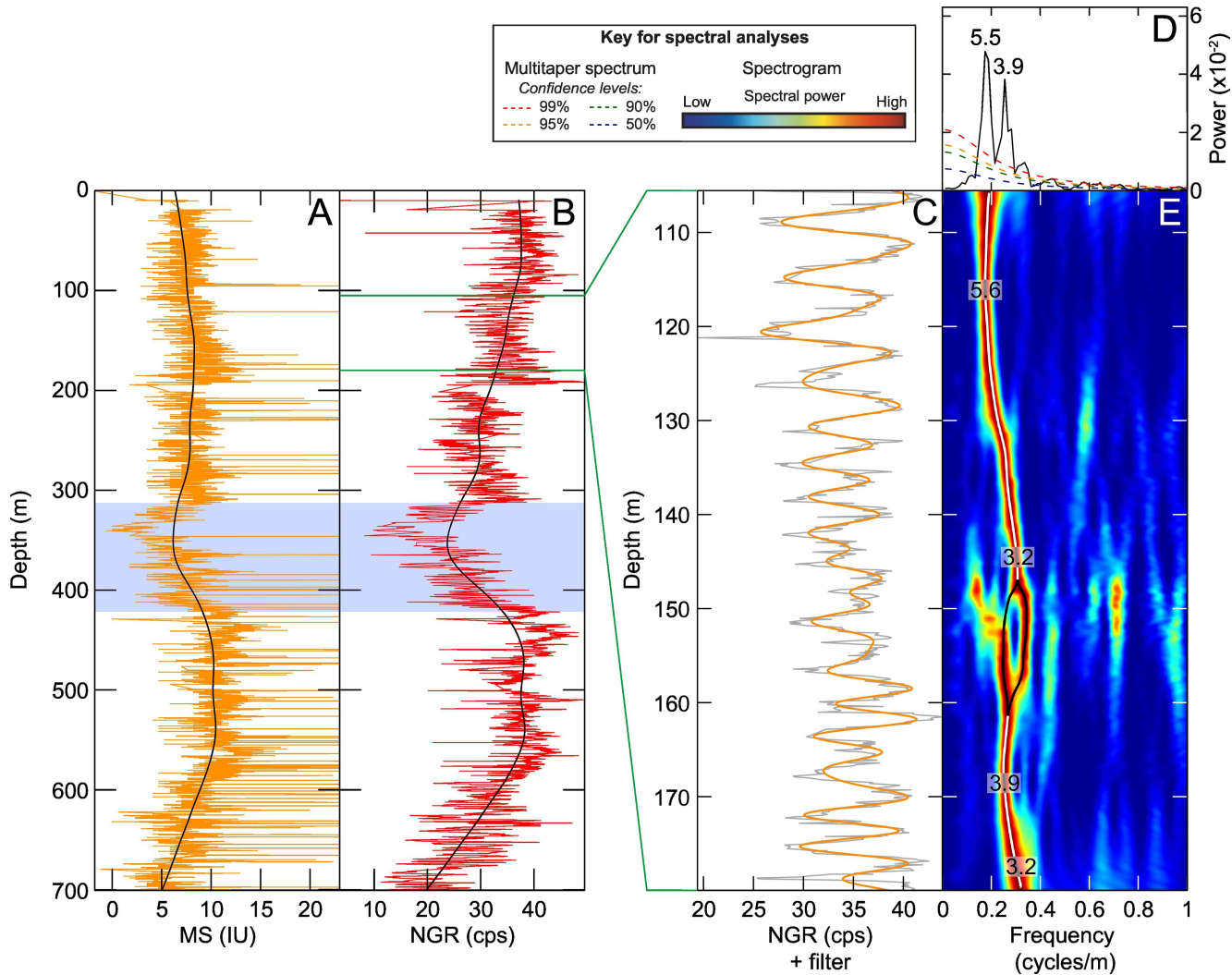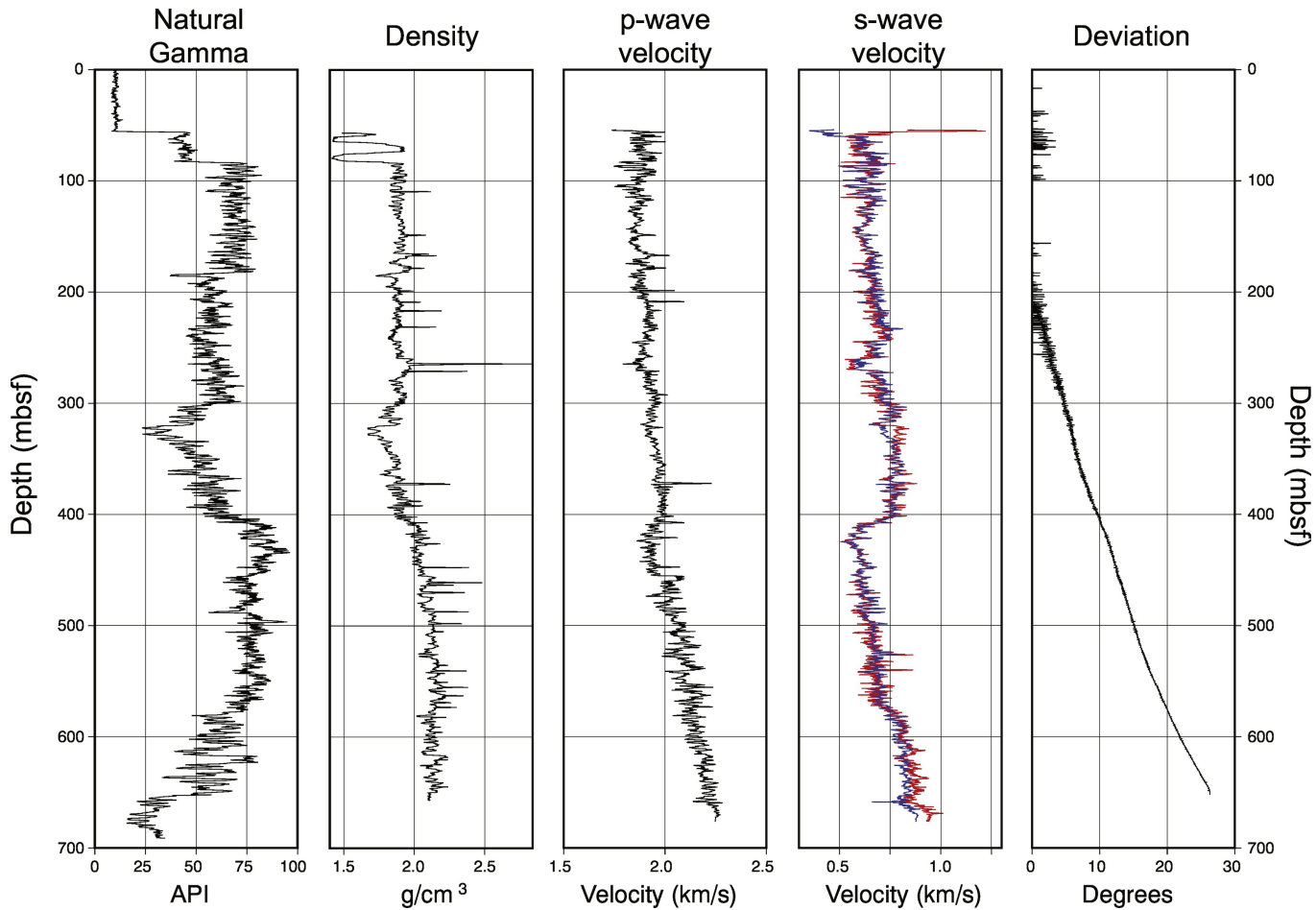| A	B	C	D	E	F
369-U1512A 4R-4, 49 - 58 cm	369-U1512A 9R-1, 25 - 34 cm	369-U1512A 10R-7, 56 - 65 cm	369-U1512A 20R-3, 135 - 144 cm	369-U1512A 23R-6, 59 - 68 cm	369-U1512A 30R-4, 140 - 149 cm

Figure 4
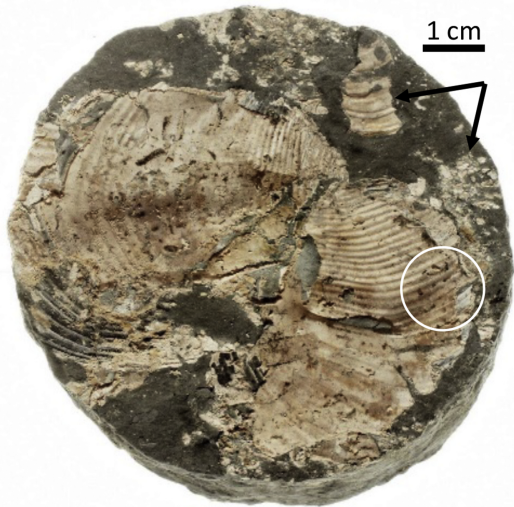
Figure 5

Figure 6

Figure 7

Figure 8